(4)

Report PME-FM-90-1

INVESTIGATION INTO THE MECHANISM OF POLYMER THREAD DRAG REDUCTION

Ronald E. Smith and William G. Tiederman
School of Mechanical Engineering
Purdue University
West Lafayette, Indiana 47907

January, 1990

Technical Report for Period 01 December 1988 - 30 November 1989

Prepared for

OFFICE OF NAVAL RESEARCH
800 North Quincy Street
Arlington, VA 22217-5000

SECURITY CLASSIFICATION OF THIS PAGE (When Data Entered)

REPORT DOCUMENTATION PAGE		READ INSTRUCTIONS BEFORE COMPLETING FORM
1. REPORT NUMBER PME-FM-90-1	2. GOVT ACCESSION NO.	3. RECIPIENT'S CATALOG NUMBER
4. TITLE (and Subtitle) INVESTIGATION INTO THE MECHANISM OF POLYMER THREAD DRAG REDUCTION		5. TYPE OF REPORT & PERIOD COVERED Technical Report for 01 December 1988 through 30 November, 1989 6. PERFORMING ORG. REPORT NUMBER
7. AUTHOR(s) Ronald E. Smith, William G. Tiederman		8. CONTRACT OR GRANT NUMBER(s) N00014-83K-0183
9. PERFORMING ORGANIZATION NAME AND ADDRESS School of Mechanical Engineering Purdue University West Lafayette, Indiana 47907		10. PROGRAM ELEMENT, PROJECT, TASK AREA & WORK UNIT NUMBERS 4322-754
11. CONTROLLING OFFICE NAME AND ADDRESS Office of Naval Research 800 North Quincy Street Arlington, VA 22217-5000		12. REPORT DATE January, 1990 13. NUMBER OF PAGES 61
14. MONITORING AGENCY NAME & ADDRESS(if different from Controlling Office)		15. SECURITY CLASS. (of this report) 15a. DECLASSIFICATION/DOWNGRADING SCHEDULE

16. DISTRIBUTION STATEMENT (of this Report)

APPROVED FOR PUBLIC RELEASE: DISTRIBUTION UNLIMITED

17. DISTRIBUTION STATEMENT (of the abstract entered in Block 20, if different from Report)

18. SUPPLEMENTARY NOTES

19. KEY WORDS (Continue on reverse side if necessary and identify by block number)

Drag reduction; polymer threads; turbulent pipe flow; concentration measurements

20. ABSTRACT (Continue on reverse side if necessary and identify by block number)

This study investigated the mechanism of drag reduction that occurs when a long chain, high molecular weight polymer is injected along the centerline of a pipe with a concentration high enough to form a coherent unbroken thread. The objective of this study was to test the hypothesis that drag reduction is caused by the diffusion of polymer molecules from the thread into the near-wall region of the pipe. The objective

DD FORM 1 JAN 73 1473 EDITION OF 1 NOV 65 IS OBSOLETE
S/N 0102-014-6601

SECURITY CLASSIFICATION OF THIS PAGE (When Data Entered)

polymer molecules from the thread into the near-wall region of the pipe. The objective was realized through the measurement of the polymer concentration in the near-wall region, the drag reduction and the radial location of the thread. The concentration was measured using a laser induced fluorescence technique where the polymer was marked with fluorescein dye.

The experiments were conducted in a 3.18 cm diameter, clear acrylic pipe at Re = 40,000 using a 5000 ppm concentration solution of Separan AP 273 as the injectant. Two centerline injectors, with diameters of 0.318 cm and 0.159 cm, were used. The near-wall, $y^+ = 50$, concentration was measured at five x/D locations, from 20 to 212, with both injectors. Drag reduction and the radial location of the thread were also measured at these five streamwise locations.

The drag reduction increased from zero at the point of injection to a maximum value about 200 diameters downstream of the injector. Maximum drag reductions of 45% and 37% were achieved with the 0.159 cm and 0.318 cm injectors respectively. The concentration at $y^+ = 50$ increased as the downstream distance increased for both injectors. The concentration increase and the drag reduction increase correlated very well. Drag reduction was not measured until low concentrations of polymer were detected at $y^+ = 50$. Drag reduction and concentration measurements at $y^+ = 50$ also were made for a set of low concentration centerline injection flows where the injectant completely diffused at Re = 40,000. The amount of drag reduction achieved in the thread flow and the diffused injection flow depended on the concentration at $y^+ = 50$. In either case, if the concentration at $y^+ = 50$ was the same, the drag reduction was approximately the same. The position of the polymer thread, as determined from a video record, remained inside a circle of $r/R = 0.9$, or $y^+ \geq 100$, for all injection cases. The experimental evidence supports the hypothesis that the polymer thread causes the drag reduction by diffusing low concentrations of polymer into the near-wall region.

TABLE OF CONTENTS

LIST OF TABLES

LIST OF FIGURES

Figure Page

Appendix
Figure

LIST OF SYMBOLS

Symbol	Description
A	fraction of available light collected
B	calibration constant for concentration measurements
C	concentration of dye
$\bar{C}$	average polymer concentration
C_{av}	average dye concentration
C_i	concentration of polymer injectant
C_m	well mixed concentration of polymer
D	inner diameter of the pipe
%DR	percent drag reduction
I_e	intensity of laser beam at a point inside the test section
I_f	intensity of the fluoresced light
I_{fb}	intensity of the background noise of the device used to measure the fluoresced light
I_o	intensity of the laser beam before entering the test section
I_{ob}	intensity of the background noise of the device used to measure the laser beam intensity
L	sampling volume length
P	probability that high concentration polymer exists in some region
ΔP_p	pressure drop during polymer injection
ΔP_w	pressure drop during water flow
R	inner radius of the pipe
Re	Reynolds number $Re = U_m D/\nu$
U_i	mass averaged velocity of injected polymer

Symbol	Description
U_m	mass averaged velocity of water
b	distance from entrance of beam in the test section to the point of measurement
d	inner diameter of the injector
f	friction factor $f = 2\frac{D}{\rho U_m^2}\frac{\Delta P_w}{\Delta x}$
g	gravitational constant
h	channel height
p	polymer type
ppm	parts per million by weight
r	radius
u_τ	friction velocity $u_\tau = (\tau_w/\rho)^{1/2}$
x	streamwise distance downstream of the injector
y	distance from the wall
y^+	distance from the wall normalized with u_τ and ν
ε	extinction coefficient of the dye
μ	dynamic viscosity of water
ν	kinematic viscosity of water
ρ	density of water
τ_w	wall shear stress
ϕ	quantum yield of fluorescence

CHAPTER 1 - INTRODUCTION

Beginning with the unexpected discovery by Toms (1948) that a few parts per million of long chain polymer molecules could reduce the turbulent drag of liquid flows, a large amount of effort has gone into understanding the mechanism behind this phenomena. The practical benefit of reducing drag on submerged bodies and inside piping and sewer networks has provided much of the incentive for studying drag reduction. The earliest experiments were carried out with homogeneous mixtures of water soluble polymers such as polyethylene oxide or polyacrylamide, or organic polymer and solvent combinations. These solutions are viscoelastic and the polymer molecules have molecular weights on the order of 10^6.

There are three basic methods for adding polymer to a turbulent flow as shown in figure 1.1. A homogeneous flow is one where the polymer has been mixed into the solvent and disperses uniformly before it is allowed to flow in a pipe. The mixture would be allowed to mix for a period of several hours. A diffusing injection flow is one where the polymer is injected into the center or at the wall of a pipe at a concentration which disperses completely by turbulent diffusion. A polymer thread flow is one where the polymer is injected into the centerline of a turbulent flow at a concentration where a coherent, unbroken thread forms at the injector and continues downstream for several hundred pipe diameters. These are the three most basic methods of adding a polymer solution to a turbulent flow. The characteristics of each of these flows will be discussed

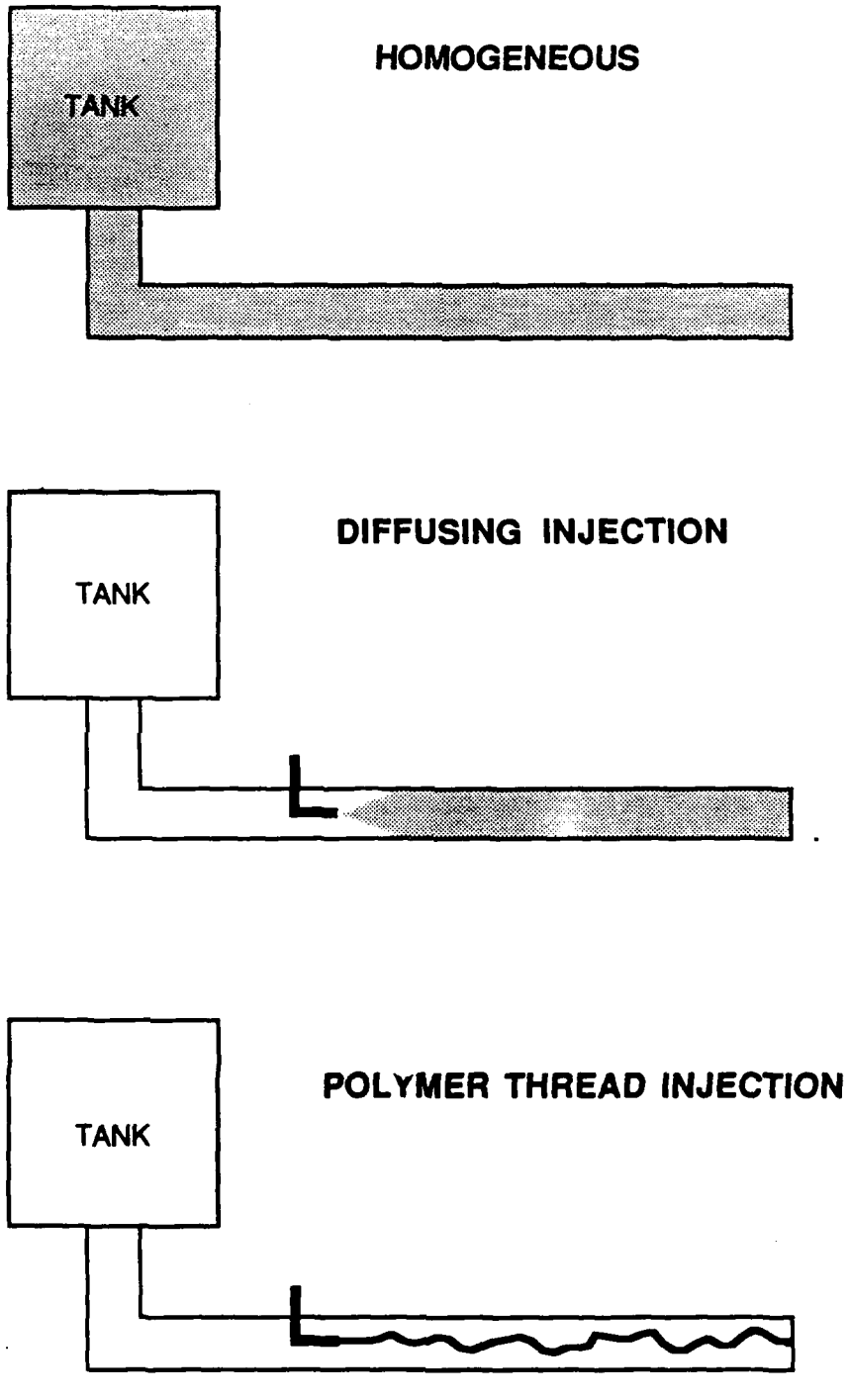

Figure 1.1 Methods of polymer addition

and compared.

The initial work in pipes with homogeneous solutions led to many discoveries about the character of drag reduction. The review by Virk (1975) contains many of the details of the early homogeneous work, a few of which will be described here. Most of these experiments were carried out in pipes with diameters less than 10 cm. For this type of flow in a pipe, the drag reduction has a distinct onset point. Through the laminar flow regime and up to a certain point in the turbulent flow regime a polymer solution with a concentration of below 100 ppm exhibits Newtonian characteristics. At a certain Reynolds number (Re) in the turbulent regime, the polymer solution begins to reduce the wall friction, or drag, as compared with a water flow at the same Re. This onset Re is a function of pipe diameter (D), polymer type (p), and mass average polymer concentration (C_m). As the pipe diameter decreases, the onset Re decreases. As C_m increases, the onset Re decreases. This onset behavior is easily detected in experiments with polyethylene oxide. The amount of drag reduction also depends on the polymer type, Re and concentration. Polyethylene oxides are generally better drag reducers than polyacrylamides of equal molecular weight. The drag reduction increases as the Re or C_m increases. The concentrations of polymer solutions in these early experiments were generally on the order of 10-100 ppm, although some experiments were conducted with concentrations as low as 1 ppm. The amount of drag reduction measured was as high as 80%.

As can be observed, most of the independent variables for polymer drag reduction are dimensional. This creates a problem in defining a universal function upon which drag reduction depends. Generally some ratio of a characteristic time scale of the

polymer solution to a time scale of the flow is suggested as an appropriate dimensionless parameter. This would eliminate the dependence on the polymer concentration, polymer type and the pipe diameter. Due to the complex rheology of these solutions, an appropriate method for determining the time scale of the solution has not been determined. As a result the functional dependence for drag reduction remains a mix of dimensional independent variables and the dimensionless Reynolds number.

Another method of introducing polymer into a flow is to inject a concentration which is low enough that the polymer disperses completely by turbulent diffusion. This type of flow is different from a homogeneous one as defined earlier and will be called a diffusing injection flow. The work of Wells and Spangler (1967) shows some of the general characteristics of diffusing injection flows. They conducted experiments in a 3.75 *cm diameter pipe*, Re = 85,000, where they injected drag reducing solutions of guar gum and polyacrylamide, P-295 a product of Stein-Hall Co., New York, through an injector on the centerline and through a slot in the wall. When injecting through the slot in the wall, drag reduction of 55% was obtained a few diameters downstream of the injector with a 100 ppm P-295 solution. The drag reduction decreased to 20% further downstream. This immediate increase that is greater than the steady value achieved further downstream is called an overshoot. When injecting on the centerline of the pipe, drag reduction was not measured until the polymer reached the wall. The drag reduction increased from this point with downstream distance as more polymer diffused to the wall. The polymer diffusion was observed by dyeing the injectant and visually observing the diffusion. The start of drag reduction coincided with the arrival of polymer at the wall.

A large amount of work has gone into understanding diffusing injection flows. It was determined in studies by McComb and Rabie (1982) and Tiederman et al. (1985) that the polymer solution must be present in the near-wall region, $10 < y^+ < 100$, for drag reduction to occur. The normalized distance from the wall is defined as $y^+ = yu_\tau/\nu$; u_τ is the friction velocity defined as $u_\tau = (\tau_w/\rho)^{1/2}$; τ_w is the wall shear stress; and ρ and ν are the density and viscosity of the water. The work of McComb and Rabie (1982) was conducted in a turbulent pipe flow with injection on the centerline and at the wall. Drag reduction as a function of downstream distance was measured for both centerline injection of a polyethylene oxide, WSR 301, and a polyacrylamide, Separan AP 30, with injectant concentrations of 1000-3000 ppm for Separan AP 30 and 500-5000 ppm for WSR 301. Only WSR 301 was injected at the wall with concentration of 500-3000 ppm. Drag reduction of up to 70% was measured for both centerline and wall injection of WSR 301. The drag reduction profiles, as a function of downstream distance, are different for wall and centerline injection. The drag reduction from wall injection increases very rapidly and exhibits an overshoot as seen by Wells and Spangler (1967). The drag reduction then settles down to a steady value. The drag reduction from centerline injection increases more slowly with downstream distance from the injector. It does not exhibit any overshoot but asymptotically approaches its maximum value.

The purpose of the McComb and Rabie (1982) study was to determine the polymer location that causes drag reduction. For this purpose, they also measured radial concentration profiles at several locations downstream of the injector. The concentration was measured by putting a known amount of salt in the injectant as a

tracer, isokinetically sampling a point in the flow with a pitot tube and analyzing the samples to determine the salt, inferring the polymer, concentration. It was assumed, from the trends observed in the drag reduction profiles, that the polymer had to exist in some annulus in order to be effective. The average polymer concentration in the annulus bounded by $15 \leq y^+ \leq 100$ was found to be directly proportional to the amount of drag reduction. This was achieved by comparing the concentration in the annulus of diffusing injection flows at points where the drag reduction was still increasing, with the concentration in the annulus of diffusing injection flows where the drag reduction had reached the asymptotic value. This was a very strong piece of evidence that the polymer molecules must be in the near-wall region in order for them to cause drag reduction.

The experiments reported by Tiederman et al. (1985) were also conducted to try to determine the polymer location that causes drag reduction. The purpose of this study was to determine if drag reduction would occur when the polymer was confined to the linear sublayer, $y^+ < 10$. The experiments were conducted in a high aspect ratio rectangular channel with injection of polymer at the wall. The injection was controlled in such a way that the polymer stayed in the linear sublayer, $y^+ < 10$, for a considerable distance. It was shown that drag reduction did not occur until the polymer solution began mixing in the $y^+ > 10$ region. The main techniques used to deduce this result were the drag reduction profile and turbulent structure information from flow visualization of the near-wall region. Both of these studies showed that for a diffusing injection flow, the polymer is only effective as a drag reducer when it is in the region, $10 < y^+ < 100$.

Since the initial discovery of drag reduction due to long chain polymers, people have tried to explain the mechanism that causes this phenomena. As has been stated, the polymer must be in the region near the wall in order to be effective. It was proposed by Gyr (1984) that drag reduction occurs when the polymer molecules are stretched. This stretching can occur if the molecules are subjected to an elongational strain. An elongational strain is produced in a turbulent flow by the turbulent bursting process in the near-wall region. It was shown by Luchik and Tiederman (1988) that the basic character of the turbulent bursting structure is not modified during drag reduction. Luchik and Tiederman also showed that the main effect of the polymer was the damping of small scale turbulent motions. They proposed an equilibrium state between the turbulent motion in the flow and the stretching of the molecules where some strong turbulent stretching from the burst event is necessary in order to keep the polymer molecules in a state where they can damp the small scale turbulent motions. This damping is caused by the viscoelastic nature of the stretched polymer molecules. A general consensus exists that polymer drag reduction is due to the stretching of the polymer molecules, but there is no direct proof that this is occurring.

There have been suggestions that drag reduction due to homogeneous flows and diffusing injection flows are not governed by the same independent variables. This can be shown by comparing the results of McComb and Rabie (1982) for diffusing injection flows with the results of Virk (1975) for homogeneous flows. Two things stand out from this comparison. The amount of drag reduction due to injection of polymer that diffuses is generally higher than that due to a homogeneous solution, especially at low concentrations and Reynolds numbers. The onset Re for a diffusing injection flow is at

a much lower value than the onset Re for homogeneous flows. It has been proposed by McComb and Rabie (1982) that the difference between the two types of drag reduction has to do with the state of the polymer molecules. In a homogeneous flow, the solution is made up of mostly single molecules of polymer mixed in the solvent. In an injection flow, it is likely that the polymer reaches the critical near-wall region, as defined by McComb and Rabie (1982), in aggregates. These aggregates are known to be present in solutions and are more effective than single molecules in reducing drag according to Dunlop and Cox (1977). They may be expected to interact with a wider range of scales than individual molecules, explaining the reduction of onset Re. The difference in the drag reduction could alternatively be due to the fact that there is less degradation of the polymer in the injection flows. The exact cause of the difference between the two types of flow has not been determined, even though it is clear that they are different. Therefore, in this work, a distinction is made between homogeneous and injection flows.

A third type of drag reduction due to polymers was first reported by Vleggaar and Tels (1973). By injecting Separan AP 30, a polyacrylamide solution, with a 5000 ppm concentration on the centerline of a water flow in a glass tube, they achieved drag reduction up to 40% with the existence of a coherent polymer thread. A coherent string of polymer formed at the injector tube and continued intact downstream. This thread was recorded from the side with a video camera and observed at Re < 30,000 to still be intact and coherent 150 tube diameters downstream of the injector. From visual observation of the video recordings, it was concluded that the majority of the polymer was not diffused from the thread. This type of flow will be called an apparently non-

diffusing or thread injection flow. The drag reduction was only measured at one point, so no understanding of the effects of downstream distance on drag reduction was gained. Bewersdorff (1982) showed a considerable effect of downstream distance on drag reduction. The drag reduction results from the thread injection flow were compared with a homogeneous polymer flow at the same C_m and Re. It was shown that the drag reduction as a function of C_m was not the same for these two flows. This was not a good comparison for two reasons. The well mixed concentration for the thread is meaningless and cannot be used for comparison because the thread never mixes fully with the solvent. There is a difference, as discussed earlier, between injection flows and homogeneous flows. The thread case, being an injection flow, should have been compared with a diffusing injection flow. A hypothesis was proposed stating that the polymer thread interacting with the turbulence in the central core flow caused the drag reduction. An alternative mechanism will be tested in this study.

Three classifications of injection of WSR 301, a polyethylene oxide, on the centerline were defined by Berman and Sinha (1984). These three classes are a) a stable, coherent, unbroken non-waving polymer thread, b) a polymer thread initially coherent and unbroken, breaking into multiple threads, and c) polymer that disperses rapidly and does not form threads. Drag reduction was seen in cases b) and c) but not in case a). The concentrations of injectant were; case a) 8000 ppm WSR 301; case b) 4000 ppm WSR 301; and case c) 500 ppm WSR 301. The type of thread that is of most interest would occur with a concentration between case a) and b) where a coherent unbroken thread, appearing to be non-diffusing to the unaided eye, produces drag reduction. This is the case where the claim was made by Vleggaar and Tels (1973) that

the thread interacts with the turbulence on the centerline to cause drag reduction.

More detailed measurements during the injection of polymer concentrations high enough to produce a thread have been made by Bewersdorff (1984). This study was done in a pipe with the centerline injection of a polyacrylamide, Separan AP 30, in the range $20{,}000 < Re < 100{,}000$. The results showed that a thread would not form until the concentration was above 3000 ppm. No thread was formed at 3000 ppm. It was also shown that the drag reduction for a thread increased from zero at the injector to on the order of 40% to 50% after 150 to 200 pipe diameters downstream, depending on Re and injectant concentration. This trend in drag reduction with downstream distance was similar to the trend seen by McComb and Rabie (1982) with the injection of polymer on the centerline that did not form a thread. The asymptotic drag reduction, when comparing a polymer thread flow to a homogeneous mixture at the same C_m, Re, D and polymer, did not agree. For a diffusing injection flow, $C_i \leq 3000$ ppm, the asymptotic drag reduction was greater than that due to a homogeneous flow at the same C_m, Re and D. For injectant concentrations, $C_i > 3000$ ppm, the asymptotic drag reduction decreased as C_i increased for the same C_m, Re and D. As C_i increased, the asymptotic drag reduction from a polymer thread was less than that from the homogeneous flow. The comparison of an injection flow to a homogeneous flow is not relevant as described earlier.

Concentration measurements, similar to McComb and Rabie (1982), were made during thread injection by the isokinetic sampling of fluid with a pitot tube. This showed that for an injectant concentration of 10,000 ppm, Re = 40,000 and 40% drag reduction, the concentration at $y^+ = 50$ was about 2 ppm. Bewersdorff did not believe

that these low concentrations were able to cause the amount of drag reduction seen in the thread case. However, McComb and Rabie (1982) achieved 35% drag reduction with a 2 ppm Separan AP 30 diffusing injection flow and 40% drag reduction with a 3 ppm Separan AP 30 diffusing injection flow at Re = 37,000. Based on the discrepancy between thread drag reduction and homogeneous drag reduction and the belief that concentrations on the order of 1 ppm in the near-wall region could not cause the levels of drag reduction seen with threads, Bewersdorff concluded that the thread must be interacting with the turbulence in the central region of the flow to cause the drag reduction. This is a different conclusion than the one reached by McComb and Rabie (1982) for the diffusing injection case. Neither of these arguments is sufficient considering the evidence cited above.

Concentration measurements based on the isokinetic sampling of fluid are not reliable as shown by Latto et al. (1981). These authors showed that the measured mean concentrations are always less than actual concentrations in injection flows when this technique is used. This is due to the strong dependence of solution viscosity upon the concentration. Because of this discovery, polymer concentration results obtained with this technique are questionable.

Two other independent variables have been proposed for polymer thread drag reduction. Bewersdorff (1989) proposed that the ratio of the velocity between the polymer and the solvent U_i/U_m has an effect on the drag reduction. It was found that as U_i/U_m was decreased, the drag reduction increased until the thread broke. At this point the drag reduction started to decrease. The other independent variables are the ratio of the inner diameter of the injector to the pipe, d/D, and the well mixed concentration,

C_m. These three variables combine to produce only two independent conditions. If two are known, the other can be calculated. The well mixed concentration is meaningless for the thread injection case, as discussed previously, so it will not be used in this study.

This discussion of the mechanism of polymer thread drag reduction, whether forced by a modification at or near the wall or caused by a modification in the central portion of the flow, is similar to the debate over the primary zone of turbulence production. There are at least two hypotheses on the origin and maintenance of turbulence. One hypothesis is that the central core drives the wall region. A second hypothesis is that the wall region drives the central core. Devices have been demonstrated to cause drag reduction that modify either the outer flow: large eddy break up devices, Savill and Mumford (1988), or modify the inner flow: riblets, Walsh and Weinstein (1979). The mechanisms by which these devices work is still under investigation.

Based on the work that has been done, an experimental program was developed with the objective to test the hypothesis that drag reduction from a polymer thread is caused by the diffusion of polymer molecules from the thread into the near-wall region of the pipe. The experiments were designed to utilize all previous experimental work that gave information about polymer threads and about regions in the flow where the polymer is effective in causing drag reduction. The experimental program consists of measuring the polymer concentration in the near-wall region, $y^+<100$, the drag reduction along the length of the pipe, and the radial location of the polymer thread when a high concentration solution of polyacrylamide, Separan AP 273, is injected along the centerline of a turbulent pipe flow. The concentration measurement, based on the technique of laser induced fluorescence, will prove whether the polymer thread

diffuses small amounts of polymer into the near-wall region of the pipe in sufficient quantities to cause the drag reduction measured. These drag reduction and concentration results will be compared with drag reduction and concentration measurements in the near-wall of a diffusing injection case at the same Re, D and polymer. The radial location measurement will be used to establish the extent of the radial motion of the thread.

Chapter two of this thesis contains a description of the apparatus and procedures that were used to achieve this objective. The theory for the concentration measurements based on laser induced fluorescence, which avoids the problems of isokinetic sampling, is derived and explained. Chapter three contains the results from the experiments. Chapter four contains the conclusions which include a new proposal for the functional dependence for polymer thread drag reduction in a pipe.

CHAPTER 2 - APPARATUS AND PROCEDURES

2.1 Experimental facilities

The water flow loop used in the experiments is shown in figure 2.1. One pump, rated at 90 gallons per minute, was used for the water flow. The pump was isolated from the flow loop by rubber couplings that reduced the amount of vibration transmitted through the piping to the measurement section. The experimental loop could be operated in either a recirculating or blowdown mode by the valves shown in figure 2.1. The initial calibration work in the pipe was done in the recirculating mode. All experiments with polymer injection were conducted in the blowdown mode because no buildup of degraded polymer and dye could be tolerated.

At each end of the pipe there was a stilling tank to isolate the measurement section from flow disturbances. These tanks are shown in figure 2.2. The upstream tank consisted of a 28 cm square Lexan box followed be a 15 cm diameter acrylic pipe. Water entered the box through a 5 cm diameter pipe perforated uniformly with 1.2 cm diameter holes. The water then passed through a plate uniformly perforated with 1.2 cm diameter holes into the 15 cm diameter pipe. The 15 cm pipe contained a honeycomb section followed by a conical section which directed the flow into another finer mesh honeycomb section. This final honeycomb section terminated in the test section. These flow manipulation devices were used to destroy any large scale turbulence that would not have decayed in the entrance length portion of the test

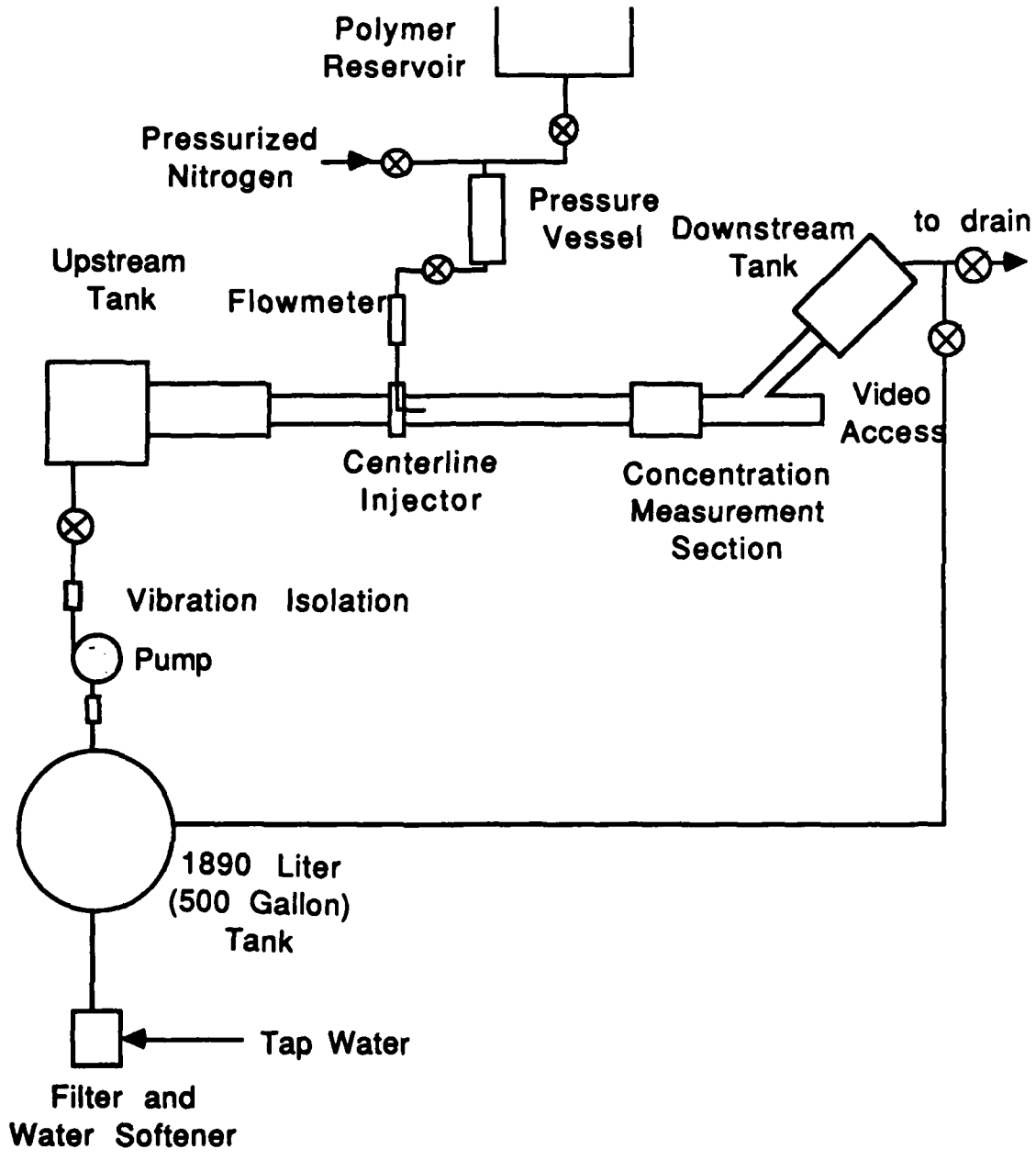

Figure 2.1 Schematic of flow loop

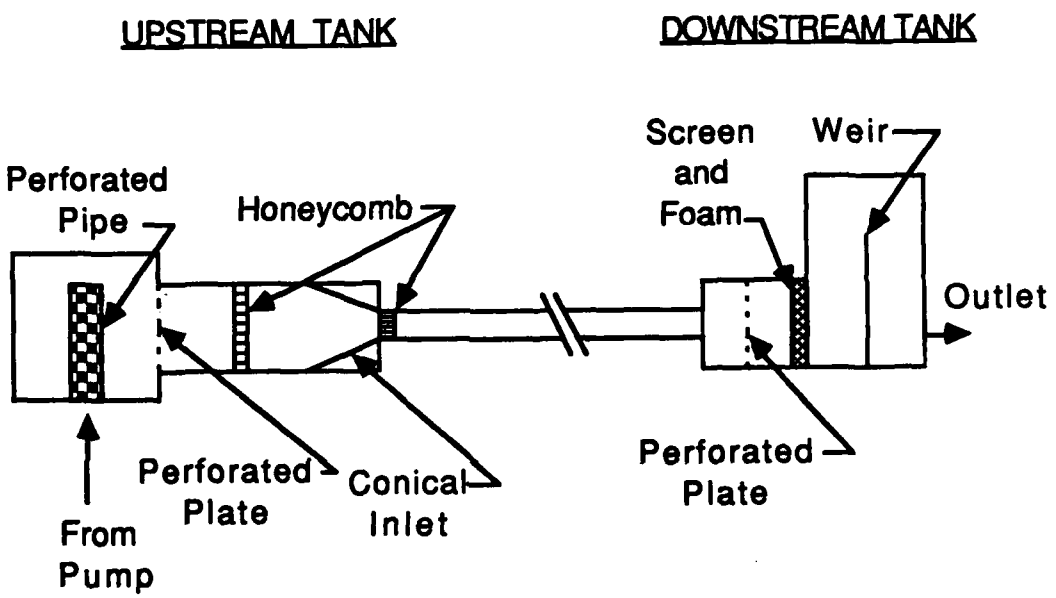

Figure 2.2 Detail of upstream and downstream tanks

section.

The downstream tank contained a perforated plate followed by a foam section enclosed in a screen. This was followed by a weir which provided a constant downstream head during the course of an experiment. The drain of the tank was on the wall facing the weir. A 10 cm diameter pipe was used to carry the fluid to the drain.

The test section, shown in figure 2.3, was a 10.4 meter long, 3.18 cm inner diameter horizontal clear acrylic pipe. The pipe was built with two 3 meter sections followed by two 1.5 meter sections that were connected with flanges. Following the 1.5 meter sections was the final 1.4 meter section which contained the concentration measurement section, the video access window and the split off to the downstream tank. The distance from the concentration measurement section to the split off to the drain was 10 pipe diameters. The concentration measurement section will be described in detail later. The injectors were constructed so that they could be inserted between any of the flanges. This provided a way to change the distance from the injector to the concentration measurement section. The first 3 meter section provided an entrance length of 94 pipe diameters upstream of the first injection point to ensure that the flow was fully developed at all points of injection.

The 3 meter section upstream of the first injection point had two static pressure taps spaced 58 diameters apart. These taps were connected to an inverted U-tube manometer. The pressure drop in this 58 diameter length was calibrated with a dump and weigh test and was used during the course of the experiment to set and hold the flow condition. The pressure taps used for the drag reduction measurements will be described in the next section.

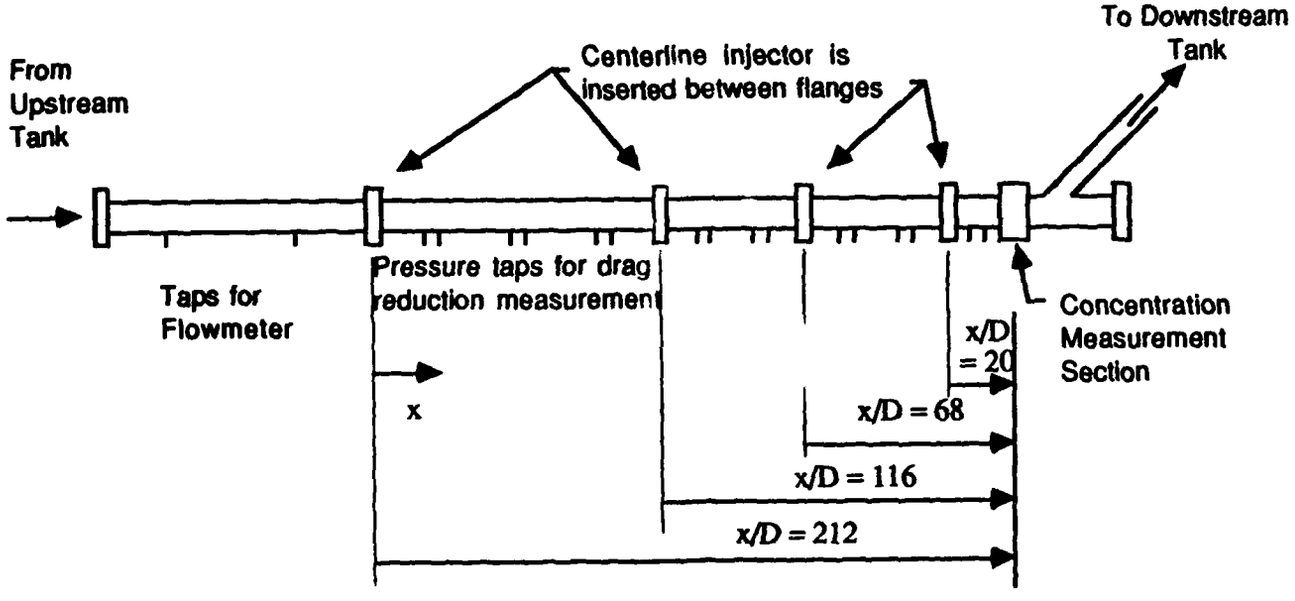

Figure 2.3 Schematic of pipe test section

Filtered, softened, deaerated water was stored in a 1890 liter (500 gallon) tank. This tank was used to hold the water for the blowdown tests.

The centerline injectors were constructed from brass tubing. The larger injector outer and inner diameters were 4.8 mm and 3.2 mm respectively. The smaller injector outer and inner diameters were 3.2 mm and 1.6 mm. This gave ratios of the inner diameter of the injector to the inner diameter of the pipe of 0.05 and 0.10.

The polymer solution used for each experiment was stored in a reservoir as shown in figure 2.1 and stirred gently when not in use. The reason for this stirring will be explained in a later section. The pressure vessel was filled with enough polymer to complete a data set and pressurized to 103 kPa (15 psi) gage just prior to conducting the experiment. The polymer flow rate was measured by a rotameter that was calibrated for each batch of polymer. This arrangement allowed the polymer to be delivered at a constant rate during the course of a data set.

2.2 Drag reduction measurement

Sixteen sets of static pressure taps were provided along the length of the measurement section. The taps in each set were spaced 12 cm apart. The pressure drop along the length of the pipe was measured with these taps using a two fluid manometer. The manometer contained water and carbon tetrachloride. The deflection of the interface between the two fluids was measured by using a needle attached to a micrometer. This device could measure pressure drops of as low as 0.015 mm of water.

Drag reduction was calculated from

$$\%DR = \frac{\Delta P_w - \Delta P_p}{\Delta P_w} \tag{2.1}$$

where ΔP_w is the pressure drop of the water flow before polymer injection and ΔP_p is the pressure drop during polymer injection at the same flow rate.

2.3 Concentration measurement

Concentration measurements were obtained in a manner similar to that of Koochesfahani and Dimotakis (1986), D. A. Walker (1987) and Walker and Tiederman (1990). The injected fluid was marked with a fluorescent dye and the intensity of the fluorescence emitted from a point along a laser beam was measured. Fluorescein sodium salt was used as the fluorescent dye. The polymer injectant was 5000 ppm Separan AP 273 which was dyed to a concentration of 8.8 ppm of fluorescein. The dye concentration at a point was determined from the fluorescent light intensity and the injectant concentration was inferred from the measured dye concentration. For turbulent flows, where dispersion occurs due to convective mixing, the turbulent mass diffusivity is typically two or more orders of magnitude larger than the molecular mass diffusivity. This indicates that the time scale for molecular diffusion is more than 100 times the time scale for turbulent diffusion. Therefore, the effect of molecular diffusion will be small and the dye concentration will yield a good estimate of the polymer concentration.

2.3.1 Analysis

For light propagating in an absorbing medium, the absorption at any differential element, dy, along the path is given by

$$dI_e(y) = -\epsilon C(y) I_e(y) dy \tag{2.2}$$

where $I_e(y)$ is the intensity of the excitation beam at point y along the path, C(y) is the dye concentration, and ε is the extinction coefficient of the dye at the excitation beam frequency. Figure 2.4 exhibits the optical set up described. The receiving path inside the pipe was very short, 0.75 mm, and the extinction coefficient of the dye is much smaller at the fluorescing frequency than at the absorption frequency, therefore the attenuation was neglected along the receiving path. The fluorescence intensity at the detector is described by

$$I_f = I_e(y)A\phi\varepsilon LC(y) \tag{2.3}$$

where $I_f(y)$ is the intensity of the fluoresced light, ϕ is the quantum yield of fluorescence, L is the length of the sampling volume along the incident beam and A is the fraction of the available light collected.

To find the equation for the beam intensity at any point along the beam with arbitrarily varying concentration, integrate Equation 2.2 along the straight beam path.

$$I_e(b) = I_o \exp(-\varepsilon \int_0^b C dy) \tag{2.4}$$

I_o is defined as the intensity of the light before it enters the measurement cell. By substituting Equation 2.4 into Equation 2.3 the fluorescence intensity at point b can be described by:

$$I_f = I_o \exp(-\varepsilon \int_0^b C dy) A\phi\varepsilon LC(b) \tag{2.5}$$

The fluorescence at any location depends on the integral, or absorption of light, along the beam path. However, at low enough concentrations or short enough beam paths

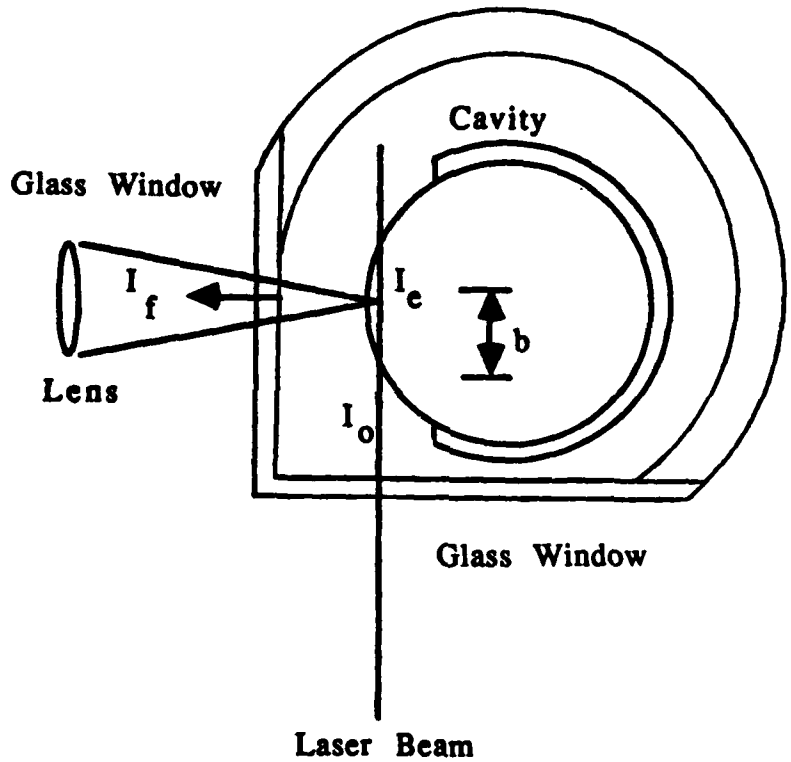

Figure 2.4 Detail of concentration measurement section, end view

$$\varepsilon b C_{av} \ll 1 \tag{2.6}$$

where

$$C_{av} = \frac{1}{b}\int_0^b C dy \tag{2.7}$$

It was shown by D. A. Walker (1987) that if

$$\log(\varepsilon b C_{av}) < -1 \tag{2.8}$$

the attenuation of the beam due to absorption was negligible. The concentrations of dye for all experiments met this condition. Therefore,

$$I_f = I_o A \phi \varepsilon L C \tag{2.9}$$

where A, ϕ, ε and L are constants of a certain dye and optical arrangement and can be determined through calibration. Rearranging Equation 2.9 yields

$$C = \frac{B I_f}{I_o} \tag{2.10}$$

where B is the constant containing the optical and dye related parameters.

For these experiments an RCA 4526 photomultiplier tube was used to measure the fluoresced radiation collected by the receiving optics. The tube output is a current that is linearly proportional to the amount of light incident on the surface of the tube offset by a dark noise level. To develop a working equation from Equation 2.10 the background level of the photomultiplier tube must be included in the equation. The light source intensity I_o was also measured by using a photodiode. This also had an output that contained a dark noise level and the light intensity level. The actual working equation that was used was:

$$C = \frac{B(I_f - I_{fb})}{I_o - I_{ob}} \tag{2.11}$$

where I_{fb} and I_{ob} are the fluorescence background and input light intensity background respectively. The constant B was determined by placing a known concentration of dye at the measurement location and measuring the light intensities. The dye concentrations that were used for calibration during the experiment corresponded to 0.5 and 5 ppm of polymer. The actual concentrations of fluorescein dye were 0.00088 and 0.0088 ppm respectively.

2.3.2 Optical arrangement

Several areas must be addressed when making optical measurements inside a clear circular tube. The main problem is deflection of the light rays due to the curved surface and index of refraction differences. To define a point in the near-wall region of a pipe, the beam was brought in vertically and the fluoresced intensity was measured horizontally as shown in figure 2.4. To minimize the effects of light steering due to the curved surface of the pipe, two things were done. The pipe wall had a thickness of 3.18 mm. A 6.3 mm wide slot was machined in the wall, as shown in figure 2.5, and covered on the inside with a 51 μm thick piece of mylar. This caused a negligible amount of deflection of the incoming beam. The mylar was attached to the acrylic pipe with a 51 μm thick piece of Scotch Brand adhesive transfer tape manufactured by the 3M Corporation. The step produced by the window is small compared to the pipe diameter. The nondimensional height of the step at Re = 40,000 is $y^+ = 7$. This is within the linear sublayer and the pipe would still be considered hydrodynamically smooth. A 7.5 cm diameter, 12.5 cm long acrylic tube with windows perpendicular to the incoming beam and outgoing fluorescence was built surrounding the slot. This produced the

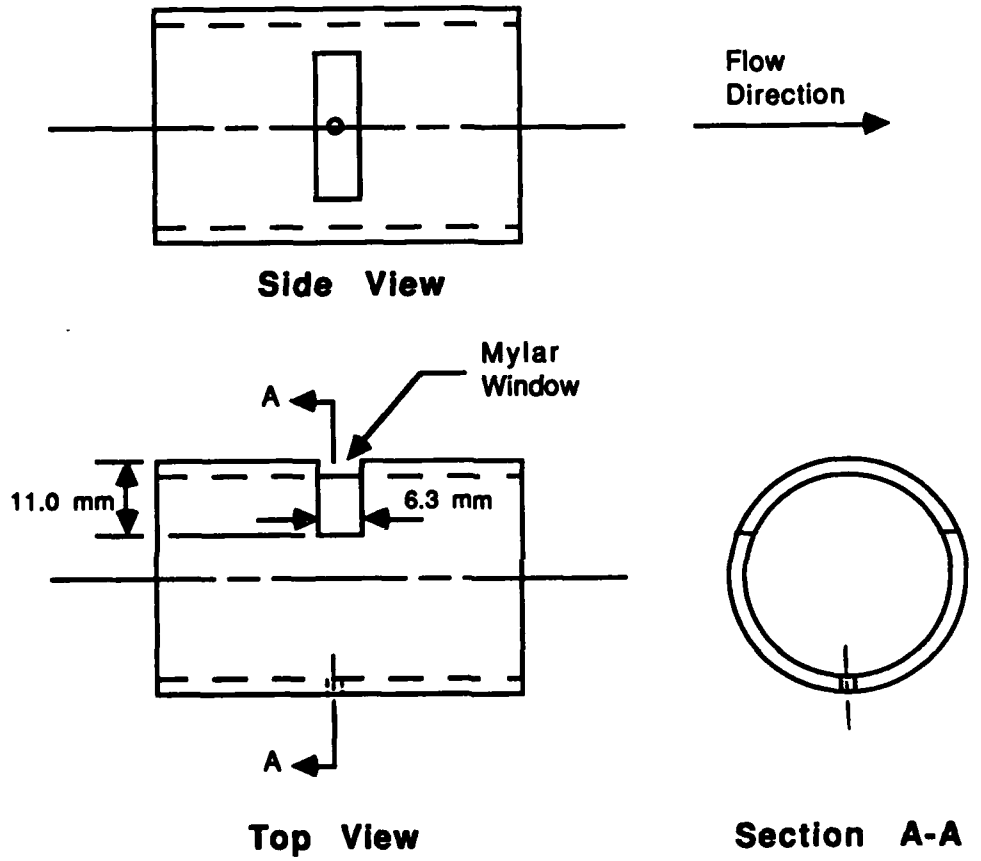

Figure 2.5 Detail of mylar window and optical access for the concentration measurement section

cavity shown in figure 2.4. The cavity was filled with the same fluid that was inside the pipe. A small hole was made in the pipe opposite the mylar window so that the pressure inside the pipe and inside the cavity was the same. These two modifications produced a minimal deflection of the incoming beam and a minimal distortion of the collected light.

The blue line (488 nm) from a Lexel model 85 Argon ion laser was used to define the point in space and to fluoresce the dye. The beam was expanded with two TSI model 9188 expansion modules and focused with a 350 mm focal length lens. This arrangement provided a beam with a diameter of 28 μm at the point of measurement. The light was collected by the optical arrangement shown in figure 2.6. A 250 mm focal length lens was used to collect the fluoresced light. The light then passed through a TSI model 9143 field stop assembly with a 200 μm aperture. The majority of the blue light was removed by a TSI model 9145 color separator. The rest of the blue light from the reflection at the window was blocked by the aperture. The collected light was then focused on a 200 μm aperture in front of the photomultiplier tube with a TSI model 9140 receiving module. The effective aperture size was 250 μm due to the size of the field stop.

2.3.3 Data acquisition

All timing and data acquisition tasks were accomplished using a Masscomp 5520 micro-computer. A block diagram of the electronic arrangement is given in figure 2.7. Data were acquired on two channels using a 12 bit A/D converter capable of one million conversions a second. The clock module of the computer was used to set the sampling rate during the data acquisition.

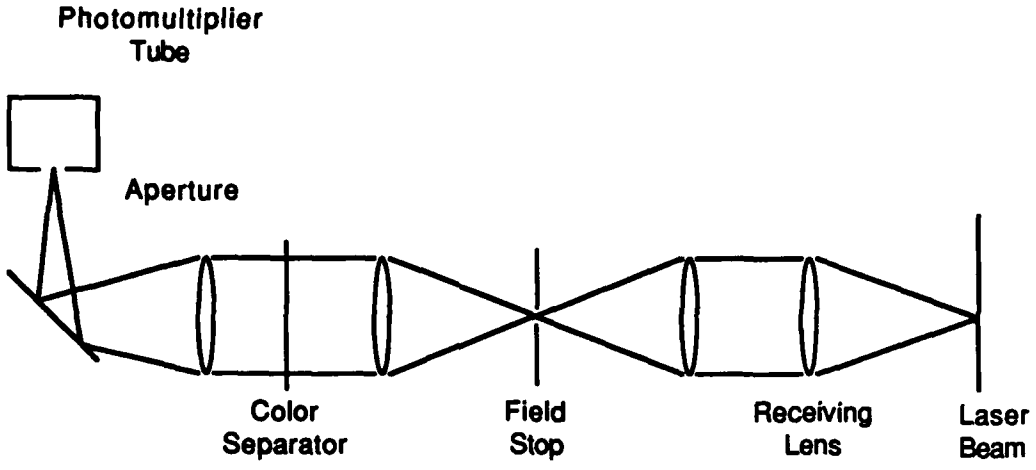

Figure 2.6 Optical arrangement for light collection

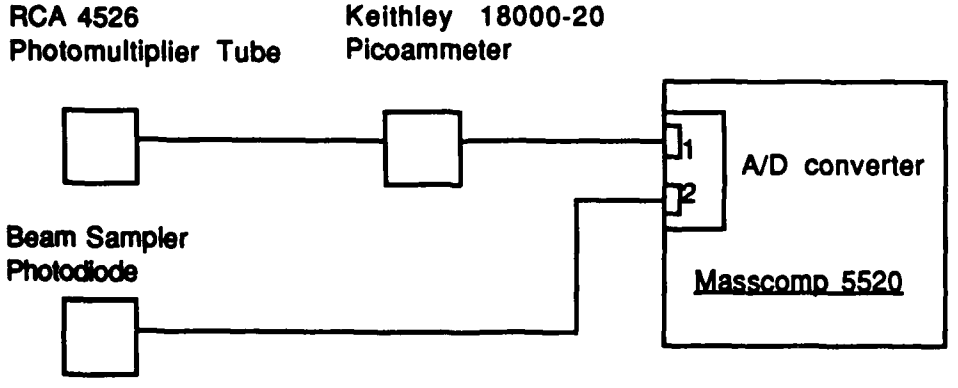

Figure 2.7 Block diagram of data acquisition arrangement

Two clocks were used in the data acquisition. One clock, the burst clock, was set at 100 kHz. This determined the time interval between the sampling of the two signals. This resulting time for sampling the photomultiplier tube and the photodiode was 10 μseconds. The other clock, the frame clock, was set at 500 Hz. This determined the rate at which the data points were taken. The data was analyzed online and checked for consistency during the course of each experiment.

The output of the photomultiplier tube was amplified using a Keithley 18000-20 picoammeter. This performed a direct current to voltage conversion over currents ranging from 10 picoamps to 10 milliamps. The response time on the scales used ranged from 700 Hz to 1.75 kHz.

2.3.4 Concentration measurement procedure

In order to measure unknown concentrations, the data acquisition set up had to be calibrated. The calibration was performed by flowing a homogeneous, known concentration solution of dyed water through the pipe and measuring the output voltages. The calibration constant was determined from the concentration and the output voltages by using Equation 2.11.

It was shown by Walker (1988) that the fluorescent emission of the dye when mixed in the polymer decreased steadily with time. It was believed that the polymers promoted the formation of non-fluorescing aggregates of dye molecules. It was demonstrated by Walker (1988) that gentle stirring of the polymer solution slowed the process enough that there was a negligible change in fluorescence during the course of an experiment. Therefore, as soon as the polymer solution was dyed, it was gently stirred until just before its use.

It was shown by Walker (1987) that the fluorescent emission of fluorescein dye is highly dependent on pH variations when the pH is less than 9.0. When the pH is above 9.0 there was a negligible amount of change in fluorescence due to pH variations. It was also shown that there was a slight temperature dependence. The polymer solutions had a pH > 9 so the water was buffered with sodium hydroxide to a pH > 9 for all experiments. The temperature of the polymer and water was held to 21 ±1°C. The pH and temperature were measured during the course of all the experiments.

Two separate measurements with the photomultiplier tube and photodiode were required before the start of every test. The background level of the photodiode was measured with the laser off. The background level of the photomultiplier tube was measured with the laser on but with no dye in the water. The calibration constant was found by measuring the outputs for a homogeneous water solution of known dye concentration.

An identical procedure was used for each test. The pressure vessel was filled with polymer from the reservoir where it was being gently stirred. The pressure vessel was pressurized to 105 kPa (15 psi) gage. The pump was turned on and the flow condition was set using the pressure drop in the flow development section. The pressure drop from the pressure taps that were used to measure drag reduction was measured with the two fluid manometer. The polymer flow was started and adjusted to the proper value. As soon as the flow stabilized, the pressure drop was measured using the same taps that were used for the water flow. While this was being done, concentration measurements and video recordings were made. Enough water could be prepared to provide a run time of 30 minutes in the blowdown mode.

2.4 Thread position measurement

The downstream end of the test section was designed so that the radial motion of the polymer thread could be observed and recorded. The outlet for the downstream tank was split off from the main pipe at a 30° angle as shown in figure 2.3. This allowed the pipe to be continued straight and terminated with a glass window. A 488 nm laser light sheet, of width less than 1 mm, was used to define a cross section at the location of the concentration measurement. An INSTAR high speed video system manufactured by Video Logic was set up to record the motion of the thread defined by the laser sheet by looking upstream through the video access window. One minute records were made at the rate of 120 frames per second for each experimental condition. These were later analyzed to obtain an estimate of the radial locations of the polymer thread.

2.5 Polymer solution preparation

The polymer injectant was an aqueous solution of Separan AP 273, a polyacrylamide manufactured by Dow Chemical. Concentrations of 5000 ppm and 466 ppm based on weight were used in the experiments. The dry powder was suspended in 300 - 500 ml isopropyl alcohol and mixed into filtered, deaerated, softened tap water at between 33 and 38 °C using a magnetic stirrer. The concentration of this mixture was 5000 ppm. This was allowed to hydrate for at least 24 hours before use. The lower concentration solution was made by diluting the 5000 ppm solution with softened, filtered tap water to a concentration of 466 ppm. This was allowed to hydrate for at least 24 hours before use.

These experiments were conducted over a several week time span using different batches of polymer solution. To ensure comparable results, the solutions were prepared

using the above standard procedure and the batches were tested for repeatability. The pH of each batch was measured. A portion of each batch was diluted to 100 ppm. This solution was allowed to flow through a 1.405 cm diameter pipe over a range of flow rates. The pressure drop was measured and the Reynolds number and drag reduction were calculated. The amount of drag reduction was compared to other batches as well as batches from previous work conducted with the same solution. Only polymer solutions which exhibited reasonable consistency in this test were used.

CHAPTER 3 - RESULTS

3.1 Experimental condition

The experimental conditions were chosen in order to test the proposed hypothesis. As discussed in the introduction, the independent variables are: x/D, downstream distance from the injector normalized with the pipe diameter; d/D, injector diameter normalized with the pipe diameter; C_i, injectant concentration; Re, Reynolds number; p, polymer type; and U_i/U_m, velocity ratio between polymer and solvent. Table 3.1 contains the experimental conditions.

Table 3.1 Experimental Conditions

x/D	d/D	C_i	Re	p	U_i/U_m
20	0.05	5000	40,000	Separan AP 273	1.1
68	0.05	5000	40,000	Separan AP 273	1.1
116	0.05	5000	40,000	Separan AP 273	1.1
164	0.05	5000	40,000	Separan AP 273	1.1
212	0.05	5000	40,000	Separan AP 273	1.1
20	0.10	5000	40,000	Separan AP 273	1.1
68	0.10	5000	40,000	Separan AP 273	1.1
116	0.10	5000	40,000	Separan AP 273	1.1
164	0.10	5000	40,000	Separan AP 273	1.1
212	0.10	5000	40,000	Separan AP 273	1.1
212	0.05	466	40,000	Separan AP 273	varied

Another variable that has been seen to be significant in homogeneous drag reduction is the mean strain rate at the wall. For the flow without drag reduction the mean strain

rate at the wall was 4082 s^{-1}.

3.2 Water flow

The pressure drop was measured along the length of the pipe to determine if it was hydrodynamically smooth. The pressure drop was measured using a water manometer that was vented to the atmosphere. The Reynolds number was determined from the upstream flowmeter and the friction factor was determined from the pressure drop along the length of the pipe. In figure 3.1 the experimental results are compared to the Blasius correlation for turbulent flow in a smooth pipe given by $f = 0.3164/Re^{0.25}$. This correlation is valid for $Re \leq 10^5$. As can be seen, the pipe is hydrodynamically smooth over the range $30{,}000 < Re < 60{,}000$. The size of the symbol is representative of the amount of scatter in the data due to uncertainty in the pressure drop measurements.

3.3 Drag reduction

Drag reduction measurements were made for all ten experimental conditions to determine the drag reduction profile along the pipe. The drag reduction profile for the injector with d/D = 0.05 is shown in figure 3.2. The drag reduction increases from zero or slightly negative values near the injector to values on the order of 45% at the furthest downstream location. The scatter of the data points is representative of the amount of uncertainty in the data. The drag reduction attains a maximum value at x/D = 200 of 45%. The drag reduction does not appear to have reached an asymptotic value where it is no longer changing with x/D. A longer pipe would be required to reach the asymptotic region.

The drag reduction profile for the injector with d/D = 0.10 is shown in figure 3.3. This profile is similar to the one from the smaller injector in that it starts at zero or

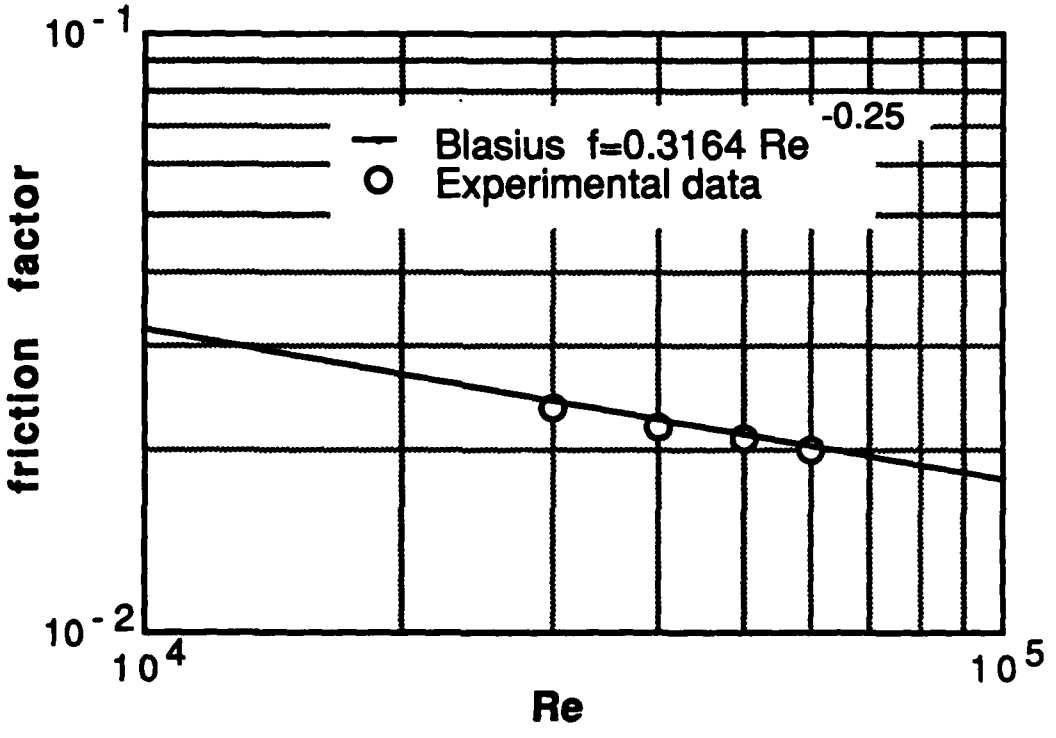

Figure 3.1 Friction coefficient for water flow

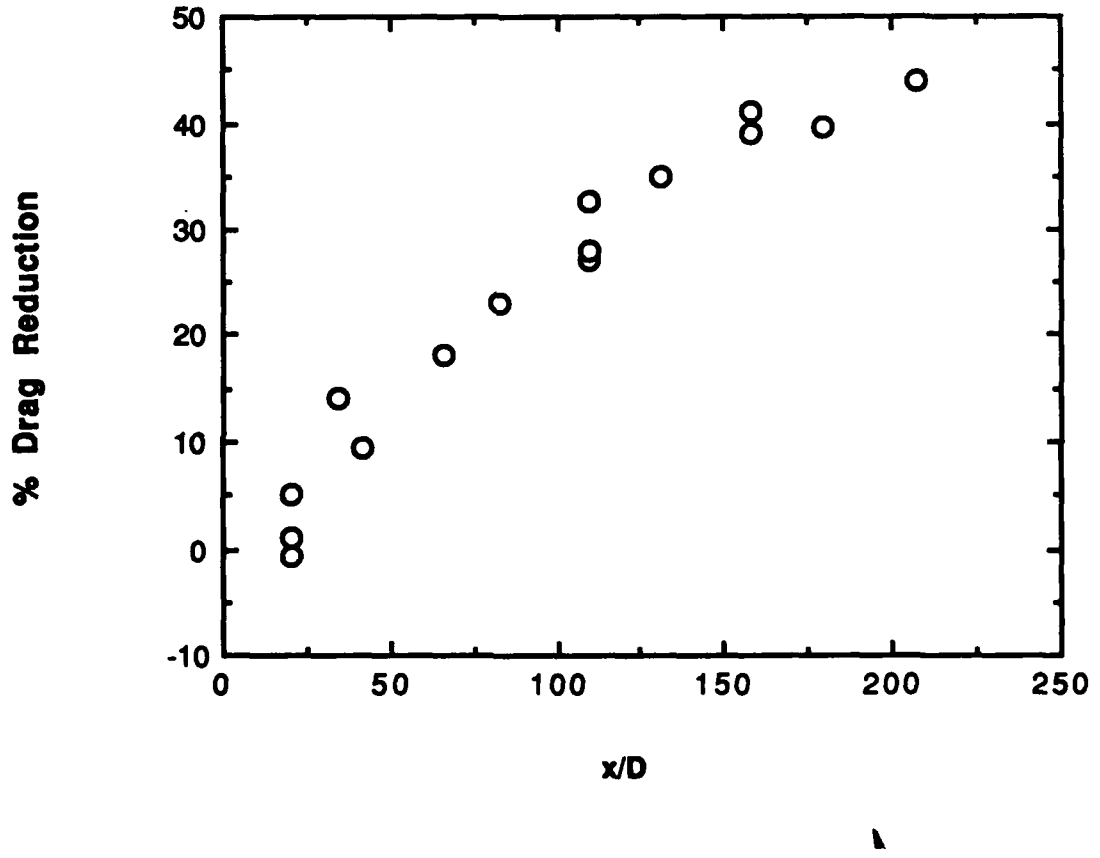

Figure 3.2 Drag reduction versus downstream distance for d/D = 0.05 injector, C_i = 5000 ppm Separan AP 273, Re = 40,000

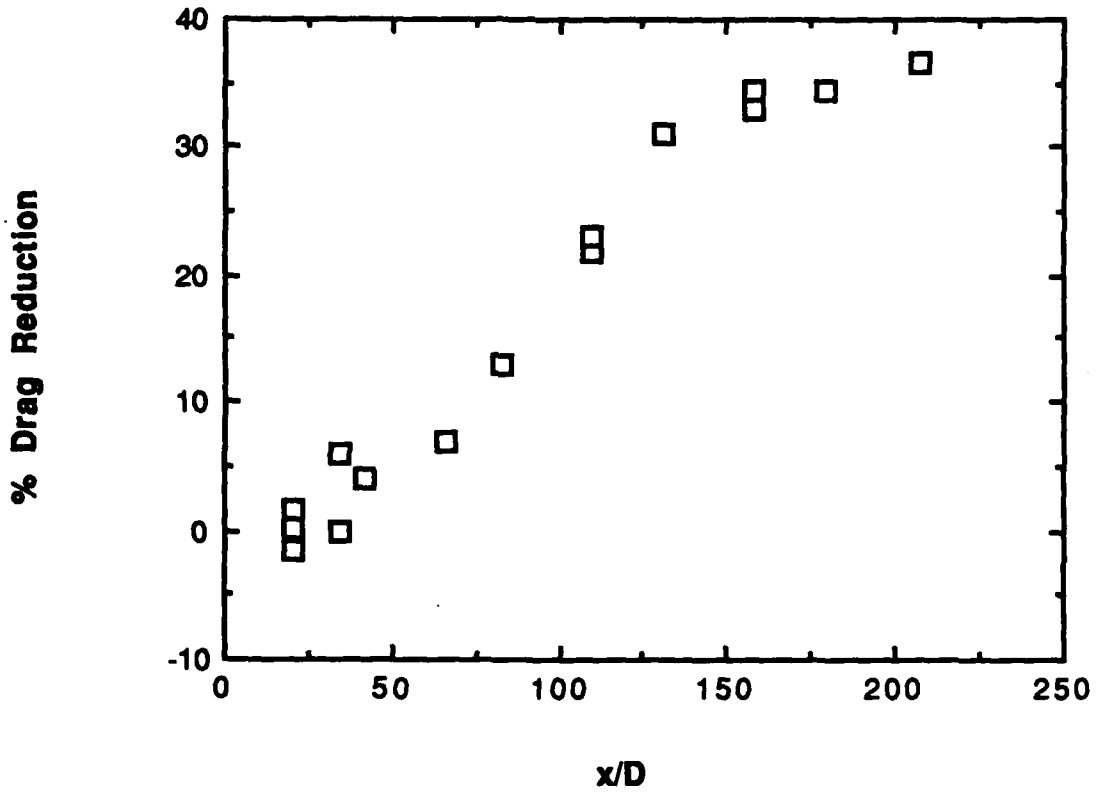

Figure 3.3 Drag reduction versus downstream distance for d/D = 0.10 injector, C_i = 5000 ppm Separan AP 273, Re = 40,000

slightly lower and increases along the length of the pipe. The increase is not as fast for the larger injector and the amount of drag reduction is not as large at the furthest downstream location. The maximum drag reduction that was seen with this injector was 37%. It also does not appear to have reached an asymptotic value. Both injectors are compared with values from Bewersdorf (1984) at essentially the same conditions in figure 3.4. The polymers that were used are slightly different, but they are both polyacrylamides. The drag reduction profiles show qualitatively good agreement over the entire range of x/D. The data from Bewersdorf seems to have reached the asymptotic value.

Prior to the experiments in the pipe a few experiments were conducted in a set of rectangular channels with polymer threads. They were run in the Reynolds number range of 20,000 - 40,000. Very small amounts of drag reduction were found using different injector configurations. These tests are described in the appendix.

3.4 Concentration measurements

Concentration measurements at $y^+ = 50$ were made for all ten experimental conditions. At all conditions, a coherent thread of polymer was observed along the entire length of the test section. The average concentration over a time period of at least 20 seconds was measured during each run. The average concentration plotted against the downstream distance is shown for both injectors in figure 3.5. The two data points at x/D = 212 for the d/D = 0.05 injector were acquired on different days with different polymer solutions. The scatter in the points is indicative of the amount of uncertainty of the concentration measurements. The concentration at $y^+ = 50$ rises from zero at x/D = 20 to about 2.5 ppm at x/D = 212. No instantaneous concentrations on the

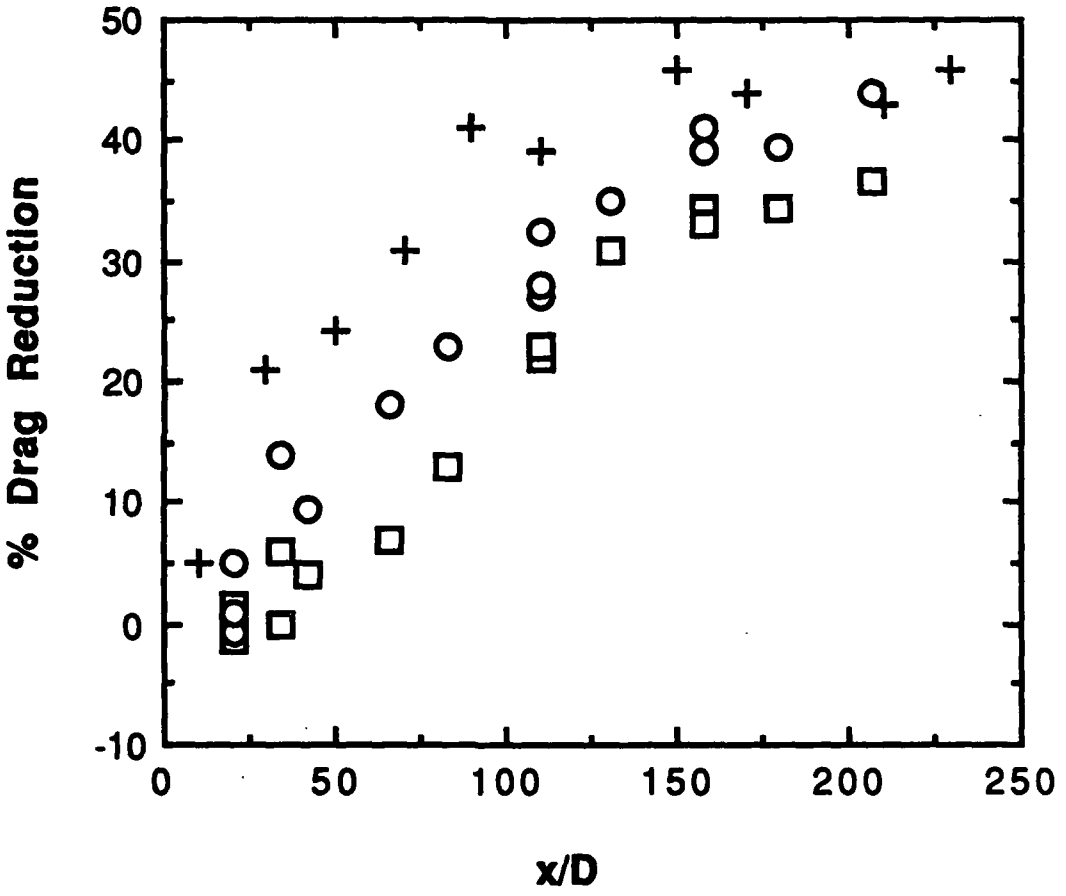

Figure 3.4 Drag reduction versus downstream distance for O - d/D = 0.05, □ - d/D = 0.10; C_i = 5000 ppm Separan AP 273, Re = 40,000; + Bewersdorf (1982), C_i = 5000 pm Separan AP 30, d/D = 0.10, Re = 40,000

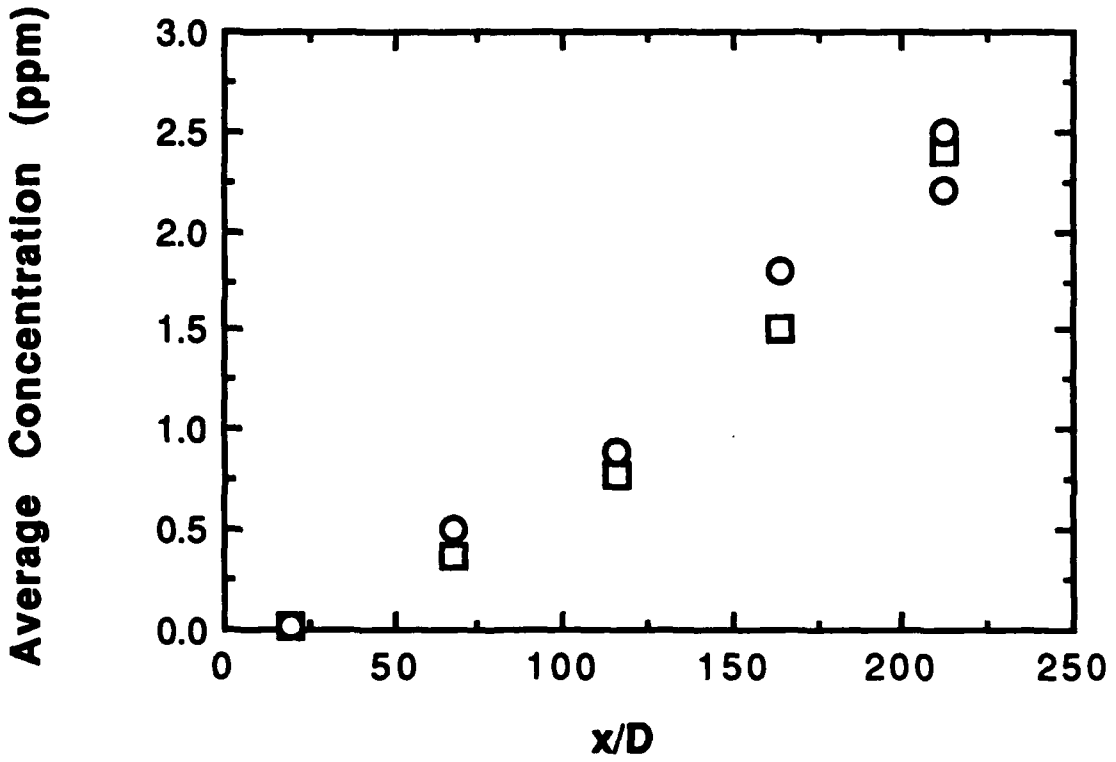

Figure 3.5 Average concentration at $y^+ = 50$, Re = 40,000, C_i = 5000 ppm Separan AP 273, O - d/D = 0.05, □ - d/D = 0.10

order of the polymer thread concentration were measured at this radial location. The highest instantaneous concentration that was measured was on the order of 20 ppm. The location of the polymer thread will be discussed further in the next section. The light levels, from which the concentration was calculated, were always at least one, and usually two, orders of magnitude greater than the background levels. There is no question, even though the concentrations are very small, that the measured light levels were from the fluorescence of the dye and not the background. The fluorescence could be seen with the unaided eye during the injection of the polymer.

Two questions arise from this measurement of near-wall concentration. When, in relation to the initial start of the thread, does this concentration appear? Is this a high enough polymer concentration to produce the amounts of drag reduction seen in the experiments or is this of secondary importance as compared to the thread? The first question was answered by observing the concentration in the near-wall region when injection was started. The concentration in the near-wall region appeared to increase from zero to the measured value at the same time that the polymer thread arrived and passed through the measurement section. This was found by observing the output from the photomultiplier tube while watching the start of the thread injection.

The second question was answered by measuring drag reduction in diffusing injection cases with these same low polymer concentrations. A test was conducted in which the polymer was injected at the centerline at a concentration of 466 ppm. This concentration of injectant dispersed rapidly and produced a low concentration, well mixed polymer flow. The drag reduction along the pipe and the concentration at $y^+ = 50$, $x/D = 212$, were measured for this flow in a manner identical to that for the

higher concentration injectant flows. Very large amounts of drag reduction were found for well mixed concentrations of polymer less than 5 ppm. A concentration of 1 ppm produced a drag reduction of over 30%. A drag reduction of 14% was measured when the concentration was only 0.23 ppm. This was the lowest flow rate of polymer that could be maintained steadily. These results were plotted along with the results from the other flows in figure 3.6. This plot shows the amount of drag reduction versus the average concentration at $y^+ = 50$. The amount of drag reduction is shown to be highly dependent on the concentration of polymer in the near-wall region.

Some of the scatter in this plot of the amount of drag reduction versus the concentration at $y^+ = 50$ could be due to the location of the concentration measurement. The measurement of concentration was only made at a single radial location. The concentration profile of the two types of injection would not be expected to be the same. The concentration of the diffused injection flow would be expected to be constant at all radial locations. The concentration profile of the high concentration polymer injection would be expected to vary from lower at the wall to much higher in the central region of the flow.

A profile of the concentration in the near-wall region $20 \leq y^+ \leq 50$ during injection of a 5000 ppm solution from the injector with d/D = 0.05 at x/D = 212 is shown in figure 3.7. As expected the concentration over this short traverse decreases slightly as the wall is approached. It will be seen later that the concentration would increase rapidly for $y^+ > 200$. The fact that the data points from the injector with d/D = 0.10 do not agree exactly with the well mixed points could be due to the difference in the concentration profile in the near-wall region. It was shown by McComb and Rabie

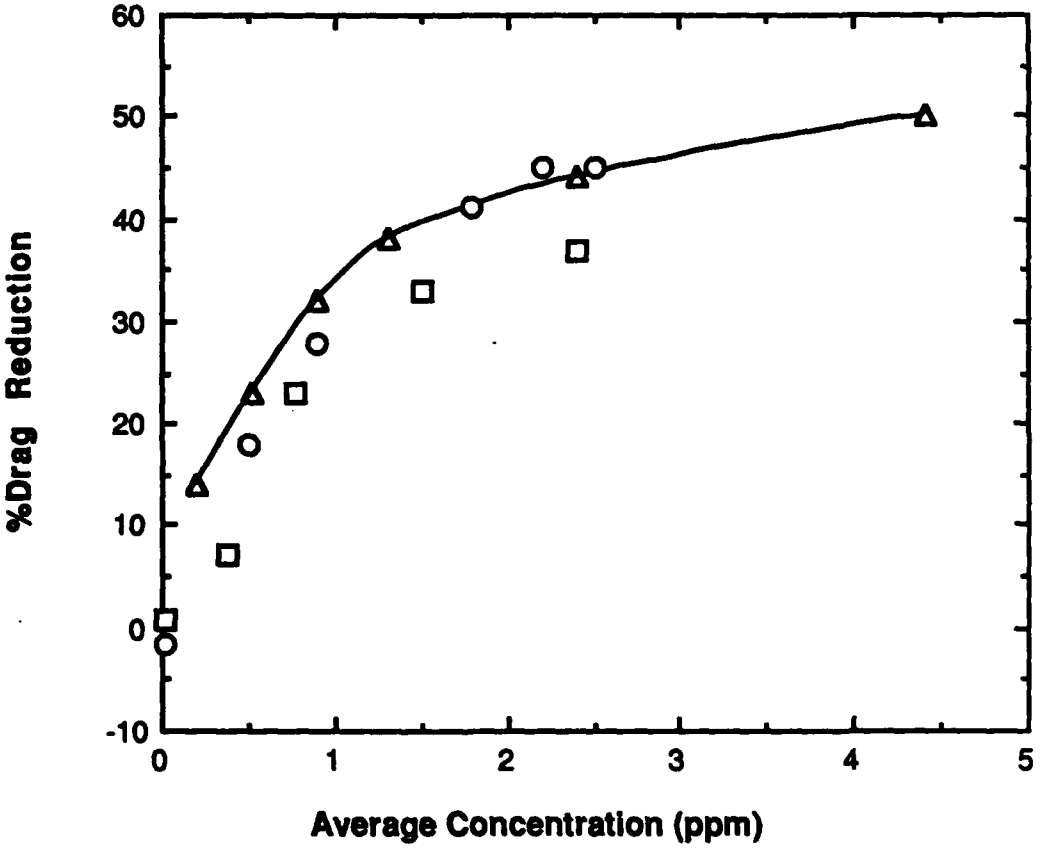

Figure 3.6 Drag reduction versus average concentration at $y^+ = 50$; Re = 40,000; O - d/D = 0.05, C_i = 5000 ppm Separan AP 273; □ - d/D = 0.10, C_i = 5000 ppm Separan AP 273; Δ, C_i = 466 ppm Separan AP 273, well mixed

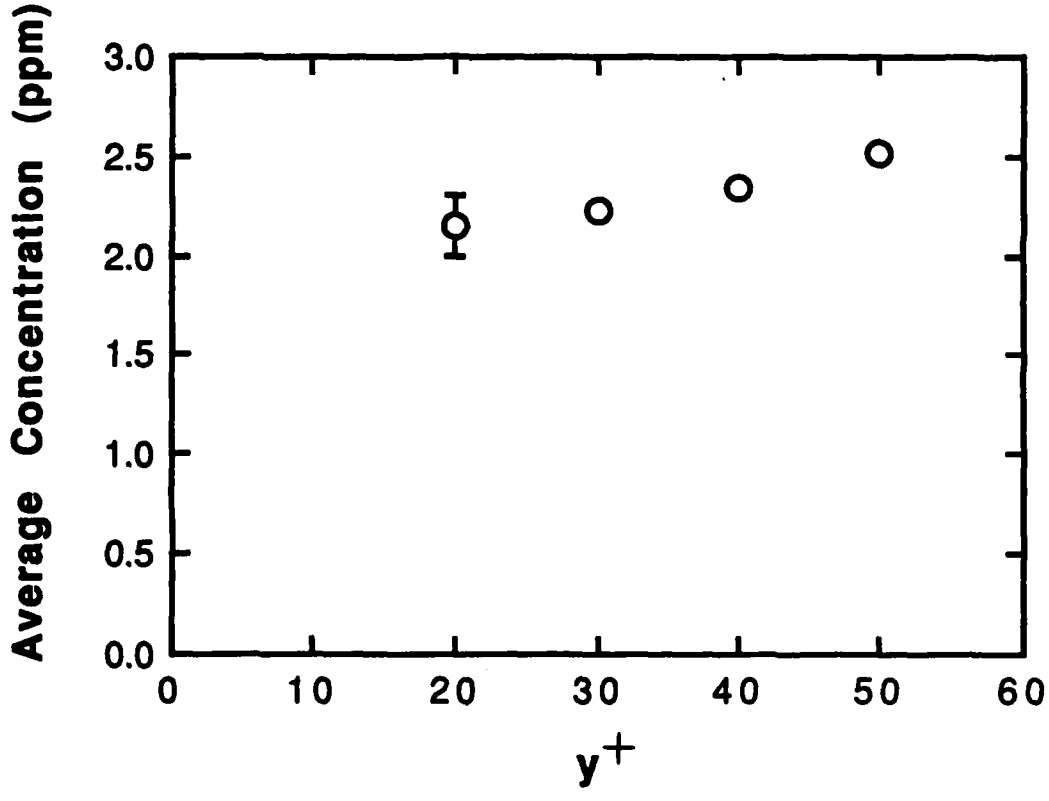

Figure 3.7 Concentration profile, x/D = 212, d/D = 0.05, C_i = 5000 ppm Separan AP 273, Re = 40,000

(1982), that the integral of the concentration in the region $10 < y^+ < 100$ and drag reduction correlated very well. The good agreement shown in Figure 3.6 is, however, a very strong piece of evidence that the mechanism of polymer thread drag reduction is very similar to, if not identical to, the mechanism for well mixed drag reduction.

3.5 Polymer thread position measurement

Video recordings were made of the motion of the polymer thread in a cross section for all ten experimental conditions. These recordings documented the radial position as well as state of the thread. Qualitative observations were made by viewing the video record in slow motion. The smaller thread (d/D = 0.05) appeared to "curl" around itself while the larger thread (d/D = 0.10) did not. These "curls" looked like "S" bends in the thread when observed from the side of the pipe. The thread remained coherent and did not break along the entire length of the pipe. Stripping of very small filaments from the thread was observed for both injection cases. These filaments were on the order of 1% - 5% of the thread diameter. The stripping for the injector with d/D = 0.05 was first observed from the video at x/D = 68. This stripping appeared to increase with downstream distance until x/D = 116. At the next point, x/D = 164, the stripping seemed to decrease while the curling of the thread increased. This corresponds to the region where the amount of drag reduction is approaching the maximum value. The stripping for the injector with d/D = 0.10 was not observed until x/D = 164. The polymer must have been diffusing from the thread prior to this point because finite concentrations were measured in the near-wall region. The injector with d/D = 0.10 created a thread that did not curl over the length of the test section. The thread was waving in the flow, but no "S" bends were observed.

Quantitative measurements were also made. A grid of concentric circles of varying radii was overlaid on the screen of the video monitor. The radial position of the high concentration polymer thread was recorded from 200 frames equally spaced over a time period of 16 seconds. Six regions were defined at radii of 20%, 40%, 60%, 80%, 90%, and 100% of the pipe radius. High concentration polymer was defined as a region of polymer with concentration at least three orders of magnitude greater than the near-wall concentration. There was no calibration of the video tape images, so this definition is not precise. The threads that were recorded on the video were very obvious and easy to spot. A region was counted once per frame if any portion of the high concentration polymer thread appeared in that region.

The probability that high concentration polymer existed outside of a circle of radius r/R plotted versus r/R is shown in figure 3.8. These data are from an x/D = 212 for both injectors. There is a zero probability that the high concentration polymer was outside a circle of r/R = 0.9. This can be shown more clearly if the probability is plotted versus the normalized distance from the wall as shown in figure 3.9. The probability of finding high concentration polymer in the region $y^+ < 100$ is zero for both injectors.

Another way to look at these results is to consider the mean strain rate variation in the turbulent pipe water flow. A plot of mean strain rate versus the normalized distance from the wall is shown in figure 3.10. This shows that the mean strain rate drops off very rapidly in the near-wall region and is quite small, $< 100\ s^{-1}$, when $y^+ > 100$. As shown by Harder (1989), drag reduction is highly dependent on the wall strain rate. For the diffusing injection case it has been shown by McComb and Rabie (1982) and Tiederman, Luchik and Bogard (1985) that the polymer must be mixed in the region

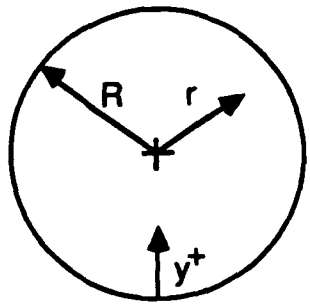

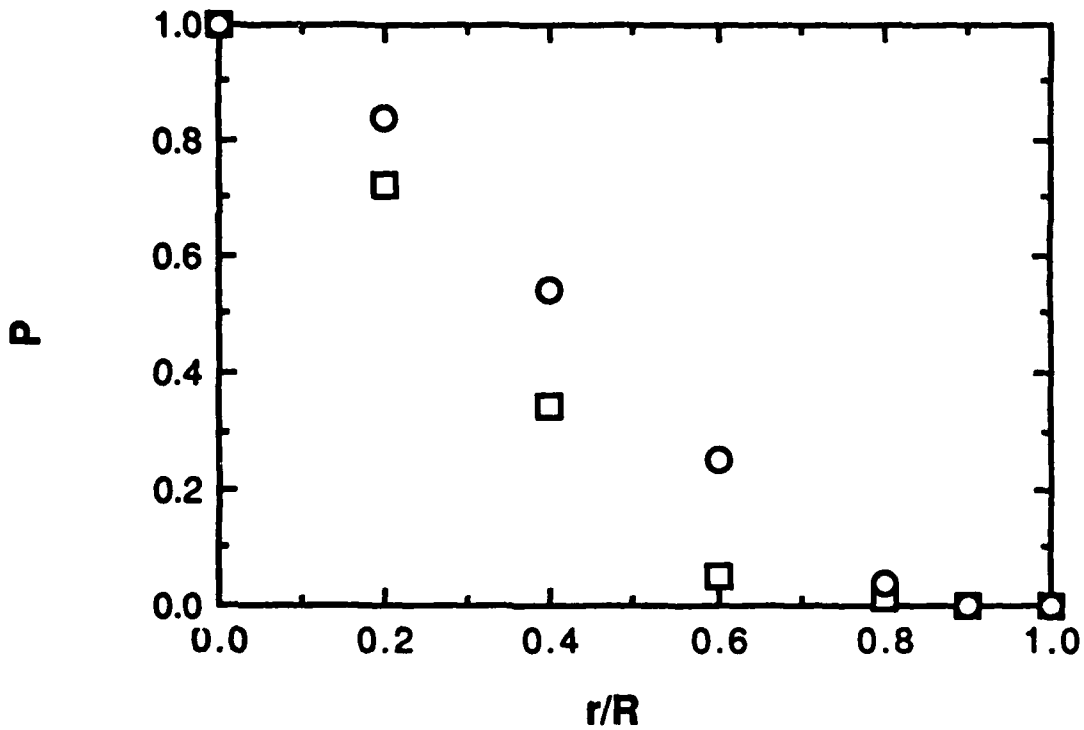

Figure 3.8 Probability that high concentration polymer exists outside a circle of radius r/R; Re = 40,000, C_i = 5000 ppm Separan AP 273, x/D = 212; O - d/D = 0.05, □ - d/D = 0.10

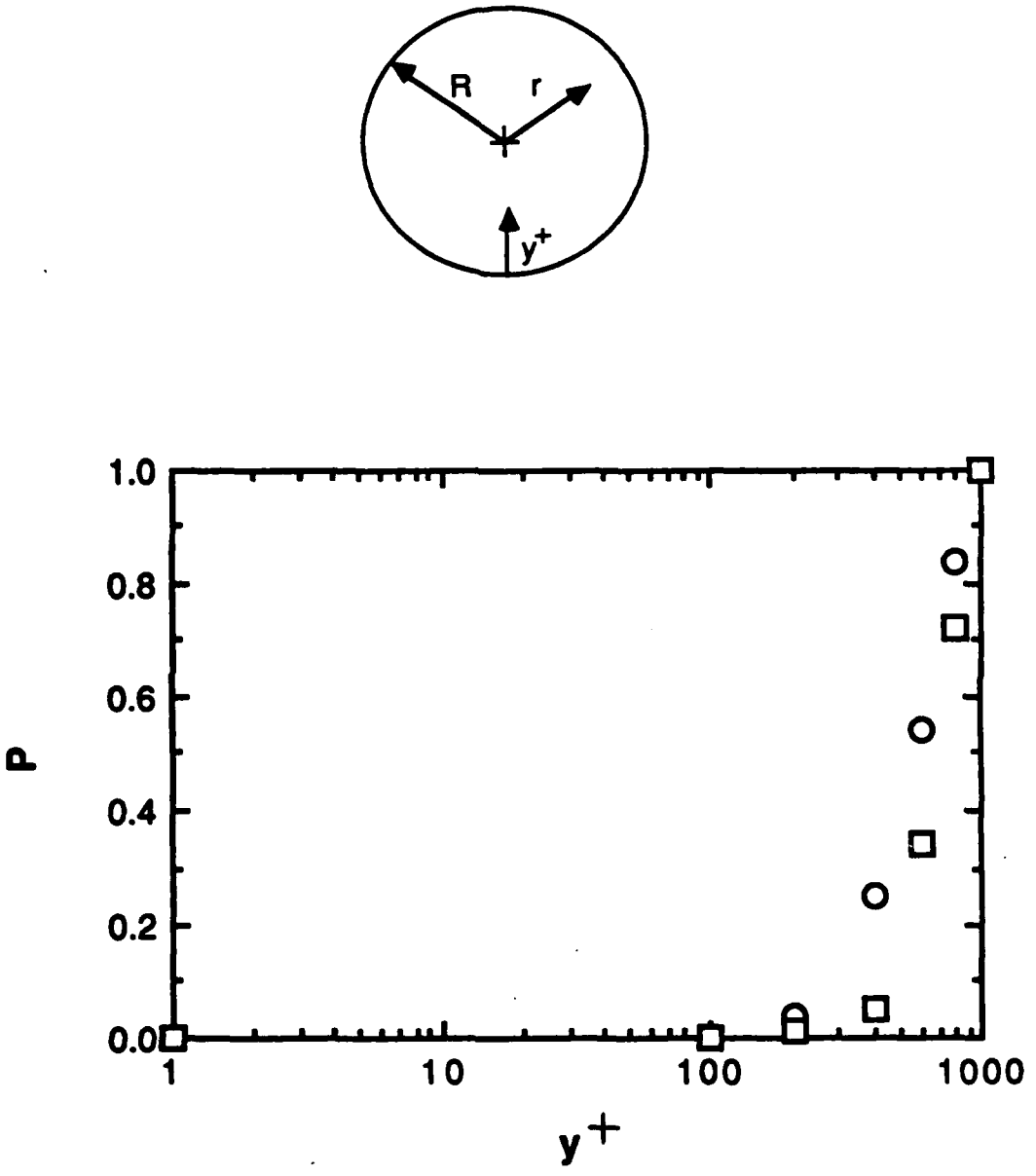

Figure 3.9 Probability that high concentration polymer exists outside a circle of radius r/R plotted versus y^+; Re = 40,000, C_i = 5000 ppm Separan AP 273, x/D = 212; O - d/D = 0.05, □ - d/D = 0.10

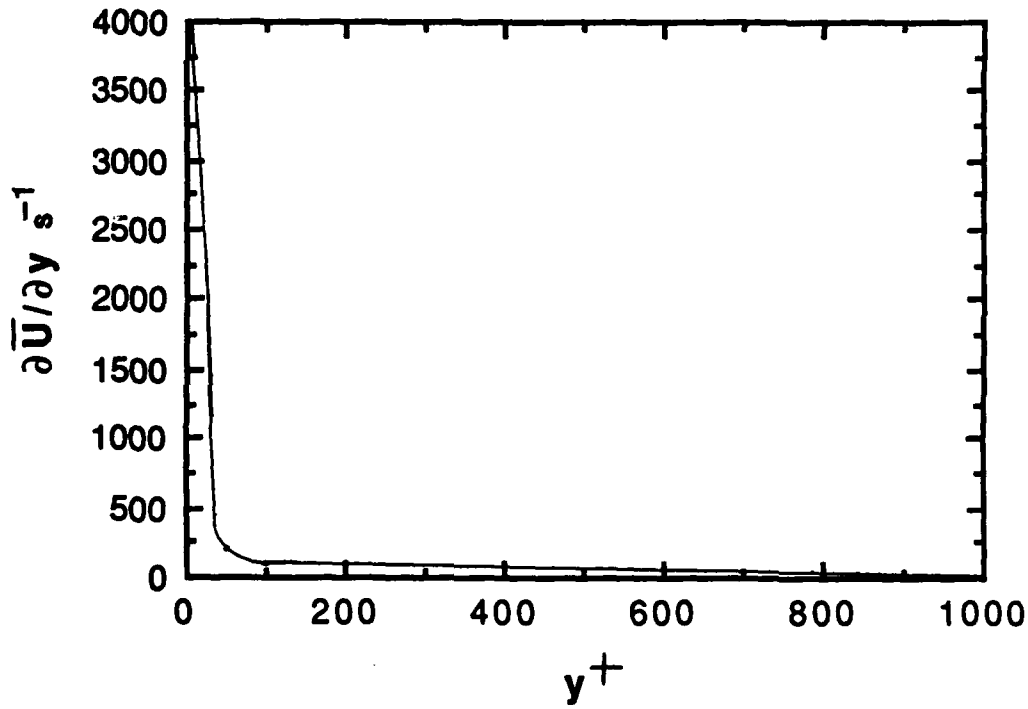

Figure 3.10 Mean strain rate versus distance from the wall, Re = 40,000

$10 < y^+ < 100$ for drag reduction to occur. This is the high mean strain rate region as seen in figure 3.10. The probability of high concentration polymer existing outside a circle of constant mean strain rate is shown in figure 3.11. This shows that the high concentration polymer spends all of its time in the low mean strain rate region, $< 100\ s^{-1}$.

In all these different ways of plotting the probability of the polymer location at x/D = 212, it can be seen that the radial dispersion of the smaller, (d/D = 0.05), thread is greater than that of the larger, (d/D = 0.10), thread. For the larger thread, the probability of seeing the polymer thread outside a given radius 10% of the time is not realized unless one is looking at a radius of 0.5 R. This means that the larger thread spends 90% of the time inside a circle of radius = 0.5 R. For the smaller thread, the probability of seeing the polymer thread outside a given radius 10% of the time occurs at 0.7 R. This difference in radial dispersion of the threads could be partially responsible for the difference in peak drag reduction observed.

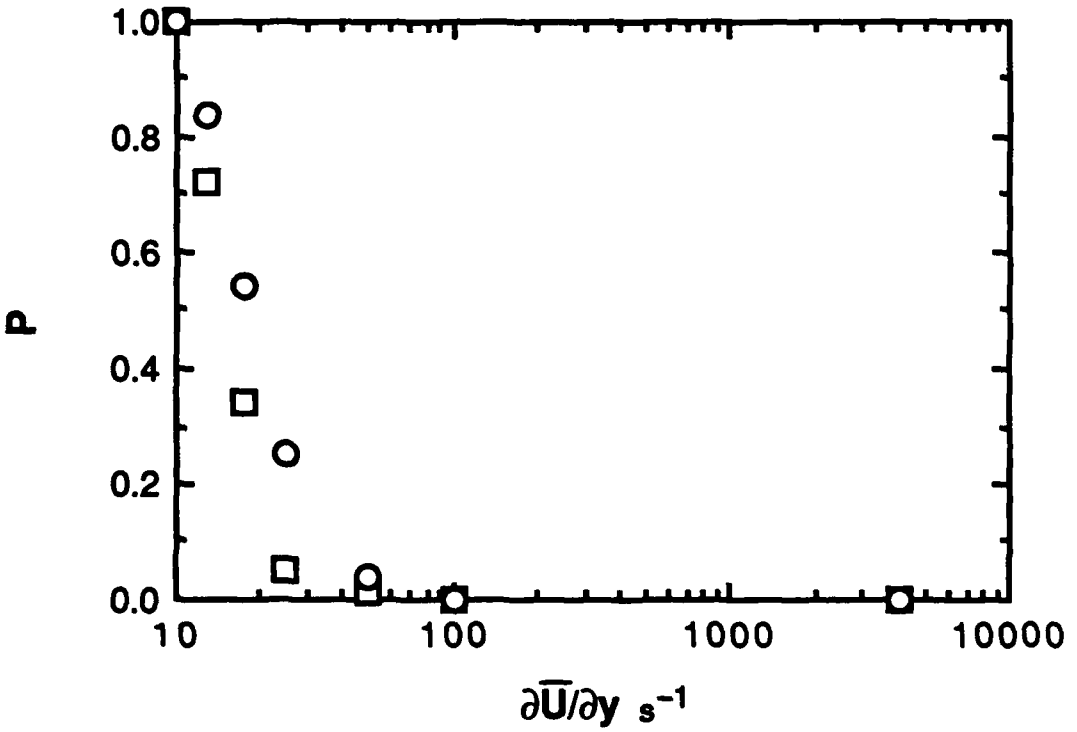

Figure 3.11 Probability that high concentration polymer exists outside a circle of constant mean strain rate; Re = 40,000, C_i = 5000 ppm Separan AP 273, x/D = 212; O - d/D = 0.05, □ - d/D = 0.10

CHAPTER 4 - CONCLUSIONS

This study of the mechanism of polymer thread drag reduction provided new insights while confirming previous results. Drag reduction was achieved with coherent threads with levels similar to those of previous experimental programs discussed in the introduction. The shape of the drag reduction curve when plotted versus the downstream distance was similar to those reported previously.

The concentration in the near-wall region and the drag reduction had the same trends with downstream distance. The concentration at $y^+ = 50$ correlated very well with drag reduction at all downstream locations. When there was no polymer at $y^+ = 50$, there was no drag reduction. As soon as measurable amounts of polymer were found at $y^+ = 50$, there was drag reduction. This was true for polymer thread flows as well as diffusing injection flows. The amount of drag reduction corresponded very well with the concentration at $y^+ = 50$ for both types of flows. Minor differences in the two different cases could be attributed to concentration gradient differences in the near-wall region.

The analysis of the video recordings provided more information about the radial displacement of the thread. The dispersion of the thread increased in the radial direction as it went downstream. However, the thread did not appear in the region $r/R > 0.9$ for any streamwise location. Another way to state this is to say that the thread did not appear in the region $y^+ < 100$ where the mean shear $> 100\ s^{-1}$. This means that

the polymer thread, as previously supposed, spends all of its time in the low mean shear central portion of the flow.

All the results support the major conclusion of this work. The existence of low concentrations of polymer in the near-wall region is sufficient to cause the drag reduction in the polymer thread experiment. This mechanism is the same one that occurs for diffused injection drag reduction. The concentration in the near-wall region is over 2000 times less than the concentration of the injectant. Nevertheless, by conducting tests with diffused injection that mixed completely at the same concentration at $y^+ = 50$ as the concentration in the thread experiments, it is clear that these low concentrations at $y^+ = 50$ can cause the magnitude of drag reduction obtained during thread injection. Therefore, polymer threads, though phenomenologically interesting, provide only a means of delivering the polymer to the near-wall region. Modification of the turbulence in the central region of the flow is not necessary to yield the drag reduction. The polymer that is diffused from the thread into the near-wall region is the major cause of the drag reduction.

From these results, it appears that there is a new simplified set of parameters that describe drag reduction due to thread injection along the centerline of a pipe. In previous investigations, polymer thread drag reduction has been compared with homogeneous drag reduction at the same Reynolds number, well mixed concentration, mean shear at the wall, and polymer type. The drag reduction results from these comparisons have not shown good agreement. If polymer thread drag reduction is compared with diffused injection drag reduction at the same Reynolds number, mean shear at the wall, polymer type and the concentration of polymer at $y^+ = 50$ the data

agree fairly well. This implies a new functional dependence for drag reduction due to injection at the centerline of a pipe.

From previous work of McComb and Rabie (1982), Reynolds number and/or mean shear at the wall appear to be important independent variables for drag reduction. Both experiments in channels, Harder (1989), and pipes with diffused injection indicate this trend. The polymer type has been proven to be a factor in the amount of drag reduction achieved. The other four variables proposed in the beginning of this work, injectant concentration, distance downstream from the injector, the ratio of injector diameter to pipe diameter and the velocity ratio between the polymer and solvent, could be replaced by some function of the concentration in the near-wall region. The concentration at a single point of $y^+ = 50$ does not appear to be sufficient to completely collapse the data, even though it did a good job considering it is only a single measurement. This is even more amazing considering that the results from the thread case where the drag reduction is developing and the polymer is actively mixing, could correspond so well with the fully developed diffused injection case. Perhaps the integral of the concentration from $10 < y^+ < 100$ as proposed by McComb and Rabie (1982) for diffused injection flows, or some functional relationship such as this could be used. The limited amount of data acquired in this study does not allow this kind of detailed analysis to be performed. However such an integral formulation would yield a new function for drag reduction due to injection of polymer addition on the centerline of a pipe of the form:

$$\%DR = f\left[\text{Re and/or } \frac{\partial \bar{U}}{\partial y_{wall}}, \text{ Polymer type, } g[\bar{C}(10 < y^+ < 100)]\right] \qquad (4.1)$$

This functional form can not be used directly because of the dimensions of the independent variables. As discussed in the introduction a characteristic time scale of the polymer solution needs to be determined from the polymer type and the concentration function. This time scale could be non-dimensionalized with the mean shear at the wall, a characteristic time scale of the turbulent flow. A workable non-dimensionalization of this form has not been discovered yet. By performing this non-dimensionalization, a universal functional dependence of drag reduction might be found.

REFERENCES

REFERENCES

Bewersdorff, H.W. 1982 Effect of a centrally injected polymer thread on drag in pipe flow, *Rheol. Acta* **21**, 587-589.

Bewersdorff, H.W. 1984 Heterogene Widerstandsverminderung bei turbulenten Rohrstromungen, *Rheol. Acta* **23**, 522-543.

Bewersdorff, H.W., 1989 Elongational effects in heterogeneous drag reduction In: *Drag Reduction 89*, Davos, Switzerland, 279-286.

Dunlop, E.H. and Cox, L.R. 1977 Influence of molecular aggregates on drag reduction. *Phys. Fluids*, **20**, s203-s213.

Gyr, A. 1984 Direct evidence that drag reduction is an effect of the elongation of polymer molecules. In: *Drag Reduction in Fluid Flows*, R.J.H. Sellin and R.T. Moses,eds. Univ. of Bristol, Paper B10.

Harder, K.J. 1989 *Influence of wall strain rate, polymer concentration, and channel height upon drag reduction and turbulent structure*. M.S. Thesis, Purdue University.

Koochesfahani, M.M. and Dimotakis, P.E. 1986 Mixing and chemical reactions in a turbulent mixing layer. *J. Fluid Mech.* **170**, 83-112.

Latto, B., El Riedy, O.K. and Vlachopoules, J. 1981 Effects of sampling rate on concentration measurements in nonhomogeneous dilute polymer solution flow. *Journal of Rheology* **25**, 583-590.

Luchik, T.S. and Tiederman, W.G. 1988 Turbulent structure in low-concentration drag-reducing channel flows. *J. Fluid Mech.* **190**, 241-263.

McComb, W.D. and Rabie, L.H. 1982 Local drag reduction due to injection of polymer solutions into turbulent flow in a pipe. Part 1: Dependence on local polymer concentration; Part 2: Laser dopler measurements of turbulent structure. *AIChE Journal* **28,** 547-565.

Savill, A.M. and Mumford, J.C. 1988 Manipulation of turbulent boundary layers by outer-layer devices: skin friction and flow visualization results. *J. Fluid Mech.* **194,** 389-418.

Tiederman, W.G., Luchik, T.S. and Bogard, D.G. 1985 Wall layer structure and drag reduction. *J. Fluid Mech.* **156,** 419-437.

Toms, B.A. 1948 Some observations on the flow of linear polymer solutions through straight pipes at large Reynolds numbers. in: *Proceedings of the First International Congress on Rheology, Holland.* II 135-141.

Virk, P.S. 1975 Drag reduction fundamentals. *AIChE Journal,* **21,** 625-656.

Vleggaar, J. and Tels, M. 1973 Drag reduction by polymer threads. *Chem. Eng. Sci.* **28,** 965-968.

Walker, D.A. 1987 A fluorescence technique for measurement of concentration of mixing liquids. *J. Phys E. Sci. Instrum.* **20,** 217-223.

Walker, D.T. 1988 *Turbulent struture and mass transport in a channel flow with polymer injection.* Ph.D. Thesis, Purdue University.

Walker, D.T. and Tiederman, W.G. 1990 *The concentration field in a turbulent channel flow with polymer injection at the wall.* Exp. in Fluids, in press.

Walsh, M.J. and Weinstein, L.M. 1979 Drag reduction and heat-transfer characteristics of small longitudinally ribbed surfaces. *AIAA Journal* **17,** 770-771.

Wells, C.W. and Spangler, J.G. 1967 Injection of a drag-reducing fluid into turbulent pipe flow of a Newtonian fluid. *Phys. Fluids,* **10,** 1890-1894.

APPENDIX

APPENDIX

Prior to the experiments in the pipe, four experiments were conducted in two rectangular channels with polymer threads. These channels had been used in prior experiments by Harder (1989) who studied well mixed, wall injection drag reduction. The highlights will be given here.

The first experiment was conducted with a single 3.1 mm inner diameter injector on the centerline of a 6 x 57 cm channel at a Reynolds number of about 40,000. The injectant concentration was 5100 ppm of Separan AP 273. This test was done to study the plausibility of forming threads and to study the motion of threads. Drag reduction measurements were not made. Video recordings were made of the thread by looking upstream at an illuminated cross section of the channel. The thread motion was recorded and analyzed. At the furthest downstream location, $x/h = 96$, the transverse thread travel was slightly over 2 channel heights. This was used as a design criteria for the next set of tests.

The next three tests were conducted in a 2.5 x 25 cm cross section channel. Three injectors were set up on the centerline, 2.5 channel heights apart in the spanwise direction so that the threads would not interact with each other. A diagram of the injector arrangement is shown in figure A.1. The purpose of these tests was to measure the drag reduction along the length of the channel. The first test was conducted with,

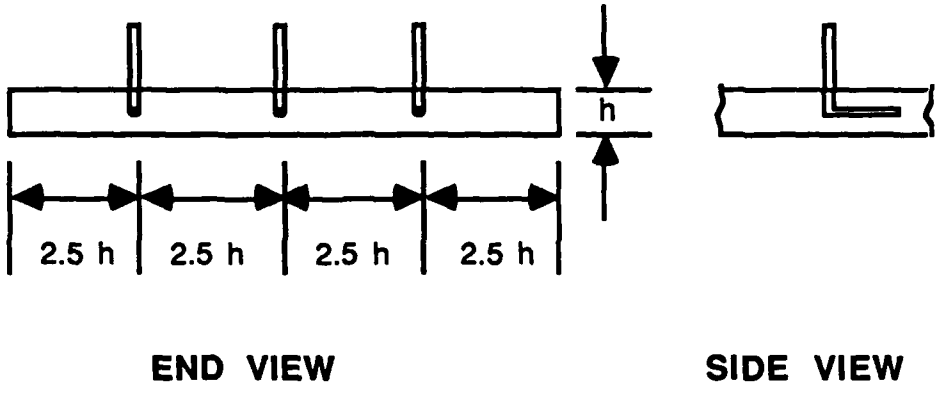

Figure A.1 Schematic of channel injector arrangement

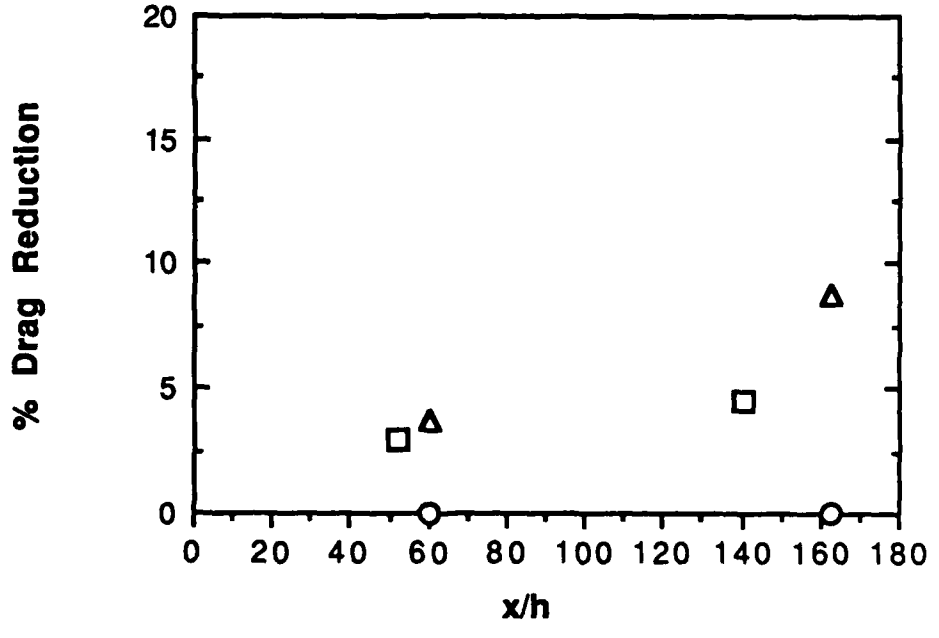

Figure A.2 Drag reduction versus downstream distance: C_i = 5000 ppm Separan AP 273, O - d/h = 0.15, Re = 18,000; □ - d/h = 0.063, Re = 23,000; Δ - d/h = 0.15, Re = 26,000

C_i = 4800 ppm, d/h = 0.063 and Re = 23,000. The inner diameter of the injectors was 1.59 mm. The injectors were sized with U_i/U_m = 1.1, the same as the injectors in the pipe experiments. The drag reduction was measured at two downstream locations as shown in figure A.2. Very low levels of drag reduction (less than 5%) were obtained.

The next two experiments were conducted with larger injectors, d = 3.81 mm. These injectors gave a d/h = 0.15. Tests were conducted at Reynolds numbers of 18,000 and 26,000. These results are also shown in figure A.2. The larger injector for this case allowed more solution to be injected. At Re = 18,000, no drag reduction was measured. At Re = 26,000, drag reduction did occur but the levels were below 10%. A plausible explanation for these results can be drawn from the work done with the pipe. If polymer has to be present in the near-wall region to cause drag reduction, then obviously in these cases the polymer did not diffuse in sufficient quantities into the near-wall region. One possible reason for this is the geometrical differences between a rectangular channel and a pipe. For the polymer threads to diffuse polymer into the near-wall region of the channel, the polymer molecules must travel further than the polymer in a pipe.

DISTRIBUTION LIST

Dr. Michael M. Reischman, Code 1132F
Office of Naval Research
800 North Quincy Street
Arlington, VA 22217-5000

Office of Naval Research
Resident Representative
536 Clark Street, Rm. 286
Chicago, IL 60605-1588

Defense Technical Information Center
Building 5, Cameron Station
Alexandria, VA 22314
(12 copies)

Mechanical Enginering Business Office
Purdue University
West Lafayette, IN 47907

Greg Anderson
Code 634
Naval Ocean System Center
San Diego, CA 92152

Prof. R.F. Blackwelder
University of Southern California
Dept. of Aerospace Engineering
University Park
Los Angeles, CA 90089-1191

Prof. D.G. Bogard
Department of Mechanical Engineering
The University of Texas
Austin, TX 78712

Dr. Steve Deutsche
ARL
Pennsylvania State University
P.O. Box 30
State College, PA 16801

Prof. T.J. Hanratty
Dept. of Chemical Engineering
1209 West California Street
Box C-3
Urbana, IL 61801

Dr. R.J. Hansen
Code 1215
Office of Naval Research
800 North Quincy Street
Arlington, VA 22217

Dr. J.H. Haritonidis
Room 37-461
Massachusetts Institute of Technology
Cambridge, MA 02139

Eric W. Hendricks
Code 634
Naval Ocean System Center
San Diego, CA 92152

Mr. G.W. Jones
DARPA/NTO
1515 Wilson Blvd.
Arlington, VA 22209

Dr. John Kim
M.S. 202A-1
NASA - Ames Research Center
Moffett Field, CA 94035

Dr. O. Kim
Code 6124
Naval Research Laboratory
Washington, DC 20375

Prof. S.J. Kline
Thermosciences Division
Dept. of Mechanical Engineering
Stanford University
Stanford, CA 94305

G. Leal
Dept. of Chemical & Nuclear Engineering
University of California
Santa Barbara, CA 93106

Justin H. McCarthy
Code 1540
David Taylor Research Center
Bethesda, MD 20084

Dr. C.L. Merkle
Dept. of Mechanical Engineering
Pennsylvania State University
State College, PA 16801

Richard H. Nadolink
Code 821
Naval Underwater Systems Center
Bldg. 679/1
Newport, RI 02841-5047

Steve Robinson
M.S. 229-1
NASA - Ames Research Center
Moffett Field, CA 94035

W.G. Souders
Code 1543
David Taylor Research Center
Bethesda, MD 20084

J.D. Swearingen
Code 4420
Naval Research Laboratory
Washington, DC 20375

Prof. David T. Walker
Dept. of Naval Architecture
and Marine Engineering
North Campus
Ann Arbor, MI 48109-2145

Prof. W.W. Willmarth
Dept. of Aerospace Engineering
University of Michigan
Ann Arbor, MI 48109